EZGİ ŞAHİN

IZMIR KATIP CELEBI UNIVERSITY

2021

IZMIR KATIP CELEBI UNIVERSITY
GRADUATE SCHOOL OF NATURAL AND APPLIED SCIENCES

PRODUCTION AND CHARACTERIZATION OF 316L AND 316L/SiC HOLLOW FIBER MEMBRANES SINTERED IN VARIOUS ATMOSPHERES

M.Sc. THESIS

Ezgi ŞAHİN

Department of Materials Science and Engineering

Thesis Advisors:
Asst. Prof. Dr. Onur Ertuğrul
Asst. Prof. Dr. Özgün Yücel

JANUARY 2021

IZMIR KATIP CELEBI UNIVERSITY
GRADUATE SCHOOL OF NATURAL AND APPLIED SCIENCES

PRODUCTION AND CHARACTERIZATION OF 316L AND 316L/SiC HOLLOW FIBER MEMBRANES SINTERED IN VARIOUS ATMOSPHERES

M.Sc. THESIS

Ezgi ŞAHİN
(Y180219002)
ORCID ID 0000-0002-3971-9974

Department of Materials Science and Engineering

Thesis Advisors:
Asst. Prof. Dr. Onur Ertuğrul
Asst. Prof. Dr. Özgün Yücel

JANUARY 2021

İZMİR KATİP CELEBİ ÜNİVERSİTESİ

FEN BİLİMLERİ ENSTİTÜSÜ

FARKLI ATMOSFERLERDE SİNTERLENMİŞ 316L VE 316L/SiC İÇİ BOŞ FİBER MEMBRANLARIN ÜRETİMİ VE KARAKTERİZASYONU

YÜKSEK LİSANS TEZİ

Ezgi ŞAHİN

(Y180219002)

ORCID ID 0000-0002-3971-9974

Malzeme Bilimi ve Mühendisliği Ana Bilim Dalı

Tez Danışmanları:

Dr. Öğr. Üyesi Onur Ertuğrul

Dr. Öğr. Üyesi Özgün Yücel

OCAK 2021

Ezgi ŞAHİN, a **M.Sc.** student of **IKCU Graduate School of Natural and Applied Sciences**, successfully defended the thesis entitled "**PRODUCTION AND CHARACTERIZATION OF 316L AND 316L/SiC HOLLOW FIBER MEMBRANES SINTERED IN VARIOUS ATMOSPHERES**", which she prepared after fulfilling the requirements specified in the associated legislations, before the jury whose signatures are below.

Thesis Advisors :

Asst. Prof. Dr. Onur ERTUĞRUL .....
İzmir Kâtip Çelebi University

Asst. Prof. Dr. Özgün YÜCEL .....
Gebze Technical University

Jury Members :

Prof. Dr. Osman Çulha .....
Celal Bayar University

Asst. Prof. Dr. Ege Anıl Diler .....
Ege University

Assoc. Prof. Dr. Mücahit Sütçü .....
İzmir Kâtip Çelebi University

Date of Defense : 25.01.2021

To my family

FOREWORD

First and foremost, I would like to thank my advisors, Asst. Prof. Onur Ertuğrul and Asst. Prof. Özgün Yücel for all helps. They quided me with their precious opinions and supports during my master's thesis and helped me by showing great devotion at every stage of my work.

I would like to thank to my dear friends, Derya Çakan and İlkgül Öksüzcan for their precious helps during experimental study.

I would like to thank to dear Chief Researcher Emrah Billur for his precious helps.

I would like to thanks to all professors in the department.

Thanks to my dear family who supported and couraged me in the decisions I made throughout my life, who gave their financial and moral support.

Thanks to Izmir Katip Celebi University, Coordination Office of Scientific Research Projects, which provided financial support on this thesis. Scientific research project number is 2018-GAP-MÜMF-0003.

And to everyone who contributed,

THANK YOU

January 2021

Ezgi ŞAHİN

Materials Science Engineer

TABLE OF CONTENTS

Page

LIST OF TABLES

Page

LIST OF FIGURES

Page

ABBREVIATIONS

PM : Powder Metallurgy

SEM : Scanning Electron Microscope

EDX : Energy-Dispersive X-Ray Spectroscopy

XRD : X-Ray Diffraction Analysis

NMP : N-Methyl-2-Pyrrolidone

PVP : Polyvinyl Pyrrolidone

PMMA : Poly (Methyl Methacrylate)

PPM : Parts Per Million

MPa : Megapascal

SS : Stainless Steel

HF : Hollow Fiber

SiC : Silicon Carbide

YSZ : Yttria Stabilized Zirconia Nanoparticles

MMCSS : Mixed Matrix Carbon Stainless Steel

CA : Cellulose Acetate

PS : Polysulfone

PP : Polypropylene

PES : Polyethersulfone

PC : Polycarbonates

PTFE : Polytetrafluoroethylene

PA : Polyamide

PVDF : Polyvinylidene Fluoride

PET : Polyethylene Terephthalate

PEI : Polyetherimide

PRODUCTION AND CHARACTERIZATION OF 316L AND 316L/SiC HOLLOW FIBER MEMBRANES SINTERED IN VARIOUS ATMOSPHERES

ABSTRACT

Stainless steel hollow fiber membranes are used as supports or particle filters for gas and liquid seperations, wastewater purification materials in environmental, chemical and waste treatment industries. The load capacity and brittleness of ceramic hollow fibers is a problem for these applications. Therefore, studies on especially stainless steel membranes increase over the past 5 years, and materials having bending strength of 300 MPa and above, good gas permeability and filtration performance have been produced as a result of these studies. The aim of the thesis is to produce hollow fiber membranes in different powder sizes, different compositions including composites and different sintering atmospheres (argon and nitrogen/hydrogen), and to examine in detail the morphological and mechanical properties of hollow fiber membranes with superior properties. In present study, porous 316L and composite (316L+SiC) hollow fiber membranes have been prepared using the dry–wet spinning process, based on phase inversion and sintered by using two different sintering atmospheres. The effects of sintering atmospheres and methods, different particle size and different compositions on samples are characterized to obtain chemical compositions, electrical resistivity, gas permeability, pore amount, average pore size and pore shape and distribution. The hollow fibers are then subjected to a 3-point bending test to determine their mechanical properties. Results of the study show that hollow fiber samples have homogeneous hollow structure and shape. Fine and mixed particle size samples give better properties. N_2/H_2 sintered samples give higher densification and lower electrical resistivity than Ar sintered 316L samples.

Keywords: dry wet spinning, sintering, composite, stainless steel

FARKLI ATMOSFERLERDE SİNTERLENMİŞ 316L VE 316L/SiC İÇİ BOŞ FİBER MEMBRANLARIN ÜRETİMİ VE KARAKTERİZASYONU

ÖZET

Paslanmaz çelik içi boş fiber membranlar, çevre, kimya ve atık arıtma endüstrilerinde gaz ve sıvı ayrıştırmaları veya partikül filtresi olarak kullanılır. Seramik içi boş fiberlerin yük kapasitesi ve kırılganlığı bu uygulamalar için bir sorundur. Son 5 yılda özellikle paslanmaz çelik membranlarla ilgili çalışmalar artmış ve 300 MPa ve üzeri eğilme mukavemetine, iyi gaz geçirgenliğine ve filtrasyon performansına sahip malzemeler üretilmiştir. Bu tezin amacı, farklı toz boyutlarında, kompozit içeren farklı kompozisyonlarda ve farklı sinterleme atmosferlerinde (argon ve azot/hidrojen) içi boş fiber membranlar üretmek ve üstün özelliklere sahip içi boş fiber membranların morfolojik ve mekanik özelliklerini detaylı olarak incelemektir. Bu çalışmada, gözenekli 316L ve kompozit (316L+SiC) içi boş fiber membranlar kuru-yaş eğirme yöntemi kullanılarak hazırlanmış ve argon ve hidrojen/nitrojen olmak üzere iki farklı sinterleme atmosferi kullanılarak sinterlenmiştir. Kimyasal bileşimler, elektriksel direnç, gaz geçirgenliği, gözenek miktarı, ortalama gözenek boyutu ve gözenek şekli ve dağılımını elde etmek için sinterleme atmosferlerinin ve yöntemlerinin, farklı parçacık boyutlarının ve farklı bileşimlerin numuneler üzerindeki etkileri karakterize edilir. İçi boş fiberler daha sonra mekanik özelliklerini belirlemek için 3 noktalı bir eğme testine tabi tutulur. Çalışma sonuçları, içi boş elyaf numunelerinin homojen boşluklu yapı ve şekle sahip olduğunu göstermektedir. İnce ve karışık partikül boyutlu numuneler daha iyi özellikler verir. N_2/H_2 atmosferinde sinterlenmiş numuneler, Ar atmosferinde sinterlenmiş 316L numunelere göre daha yüksek yoğunluk ve daha düşük elektrik direnci sağlar.

Anahtar sözcükler: kuru-ıslak eğirme, sinterleme, kompozit, paslanmaz çelik

1. INTRODUCTION

1.1 Aim and Objective of the Thesis

Stainless steel hollow fiber membranes have gained popularity and are used in order to improve the low strength and brittleness of ceramic membranes. However, the structure and properties of these materials are extensively studied and the mechanical properties are still not at the desired level. The aim of the thesis is to produce hollow fiber membranes in different powder sizes and different compositions including composites, and to examine in detail the morphological, mechanical and gas permeability properties of 316L and 316L/SiC hollow fiber membrane materials. Also, two different sintering atmospheres (nitrogen/hydrogen and argon based) were used in conventional sintering method. As a result, it is aimed to achieve better gas permeability and to obtain products with improved flexural strength and pore size distribution.

Here, both the former successful results with the sintering atmosphere optimization as well as the successful results of 316L/SiC composite system in recent years encourage the content of the study. At the end of the thesis, the results of pure 316L samples and 316L/SiC samples will be handled independently, discussed in detail and then compared with each other. The effects of different sintering atmospheres will also be discussed. The desired result can be achieved with sufficient support for mechanical properties (bending strength), support for separation of gas and liquid with high gas permeability, or particulate filter, wastewater treatment materials. These materials are that may be of interest for industries such as the environment, chemistry and waste disposal.

1.2 Theoretical Background

1.2.1 Membranes

Membranes, as shown in Figure 1.1, allow some components in a solution mixture to pass through them. For this reason, membrane is defined as a semi-permeable barrier and Figure 1.2 shows the working principle. The separation process depends on both the chemical and physical properties such as pressure, chemical potential, size, and shape of membranes [1]. According to which parameters the properties of membranes change are shown in Figure 1.3. Membranes are used for separation of industrial gases, purification of water, ion separation in electrochemical processes, and dialysis of blood and urine [2].

Figure 1.1 Hollow Fibers [3]

Membranes are divided into two groups that are organic (polymeric) and inorganic (ceramic or metal) membranes [4]. Membranes should be produced with appropriate mechanical strength and high permeability. Thickness of membrane is directly proportional to membrane resistance and high packing density exhibited a high selectivity but, a very low diffusivity, also very low permeability [5]. Therefore, more pore density increases permeability but large diameter pore size decreases selectivity.

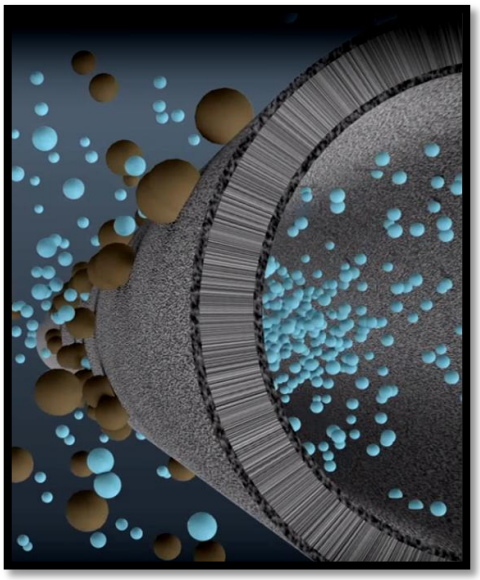

Figure 1.2 Working Principle of Hollow Fibers [6]

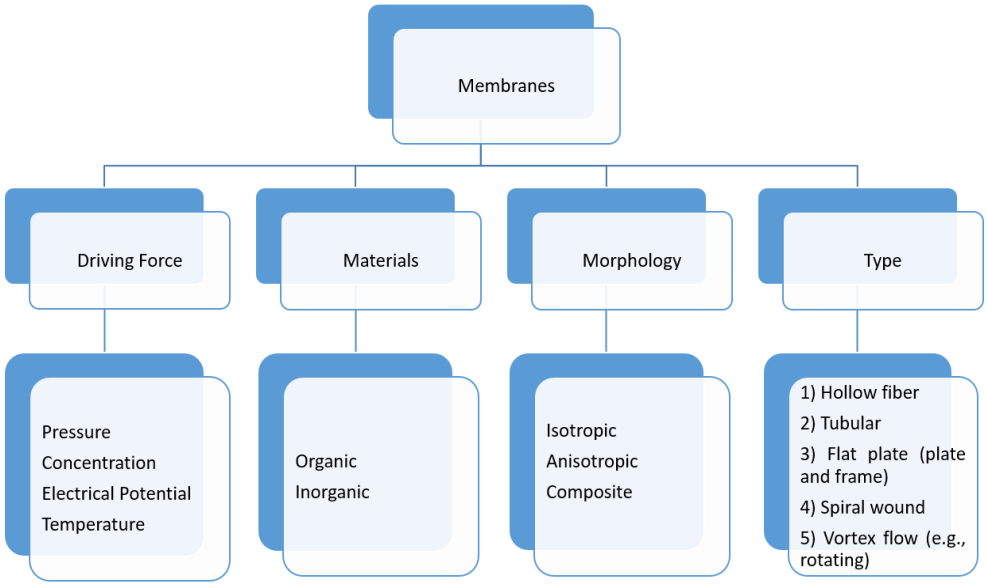

Figure 1.3 Schematic of Membranes

If the separating layers have homogeneous structure, it is called as symmetric or isotropic membrane. Symmetrical membranes have a structure with or without voids [7]. Asymmetric membranes have a non-uniform structure [8]. Composite membranes are manufactured by adding a thin layer to the top of asymmetric membranes as shown in Figure 1.4.

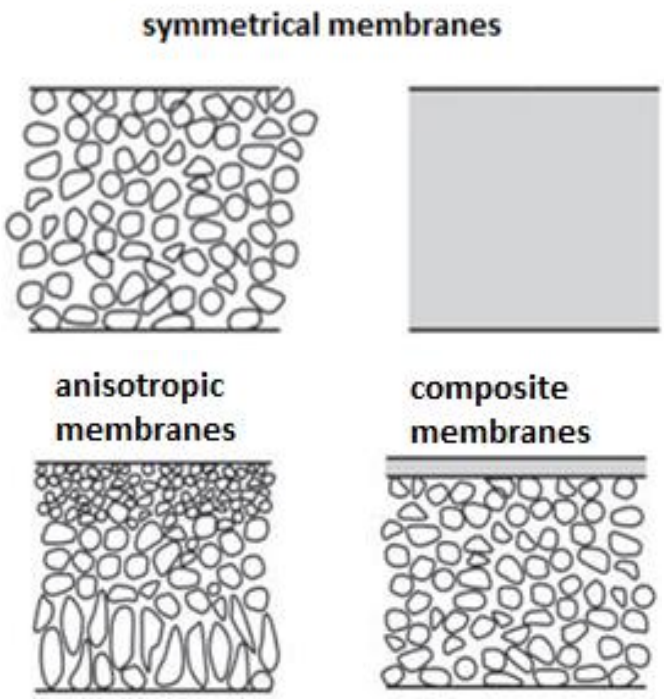

Figure 1.4 Structure of membranes

The asymmetric micro porous membranes have better performance than symmetric ones. Asymmetric membranes are operated with the largest pores facing upstream. The larger pores are pre filter to the smaller pores, so they hold larger particles at the surface but let smaller particles to enter the pore structure [9]. Filtration membranes are divided into four different categories which are microfiltration, ultra filtration, nano filtration, and reverse osmosis [10]. Porous membranes are used for microfiltration (0.1-10μm pore diameters) and ultra filtration (0.1-0.01μm pore diameters) and non-porous membranes are used for nano filtration (0.01-0.001μm pore diameters) and reverse osmosis (0.1-1nm pore diameters) processes. Microfiltration is used to remove fats and large macromolecules. Ultra filtration is used to remove of bacteria, some viruses, and to concentrate of proteins and juices. Nano filtration and reverse osmosis membranes are used in desalination applications [11]. Also, in order to provide sufficient flux, pressure increases to 1-5 bar for MF and UF, 5-10 bar for NF and 10-100 bar for RO membranes [12].

1.2.2 Hollow Fiber Membranes

Flat-frame, tubular, spiral-winding and hollow fiber (HF) membrane modules are the most commonly used configurations today for membranes as shown in Figure 1.5 [13].

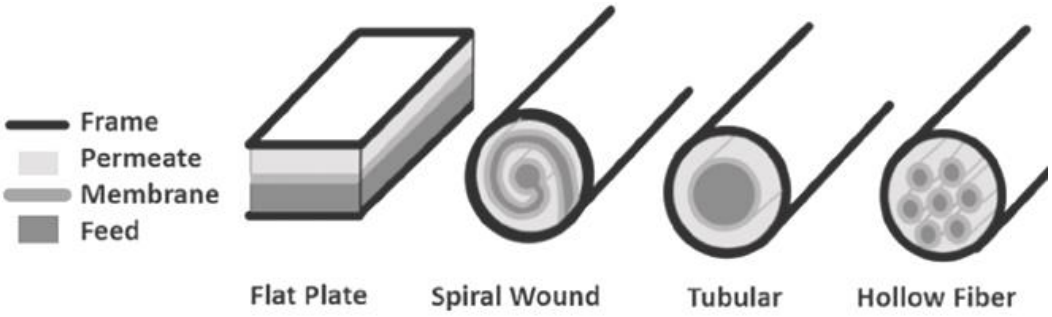

Figure 1.5 Membrane Modules Types [14]

HF membranes have advantages over other configurations. They have more surface area to unit volume due to the high packing density so they filter large volumes with minimum energy. They are capable of backwashing so they operate with high recovery [15]. Figure 1.6 represents the diameters of HF membranes. Thin (diameter of 50-200 μm) hollow fiber is used in high pressure processes. Diameter of 200-500 μm is suited for low pressure gas separation, hemodialysis and ultra filtration.

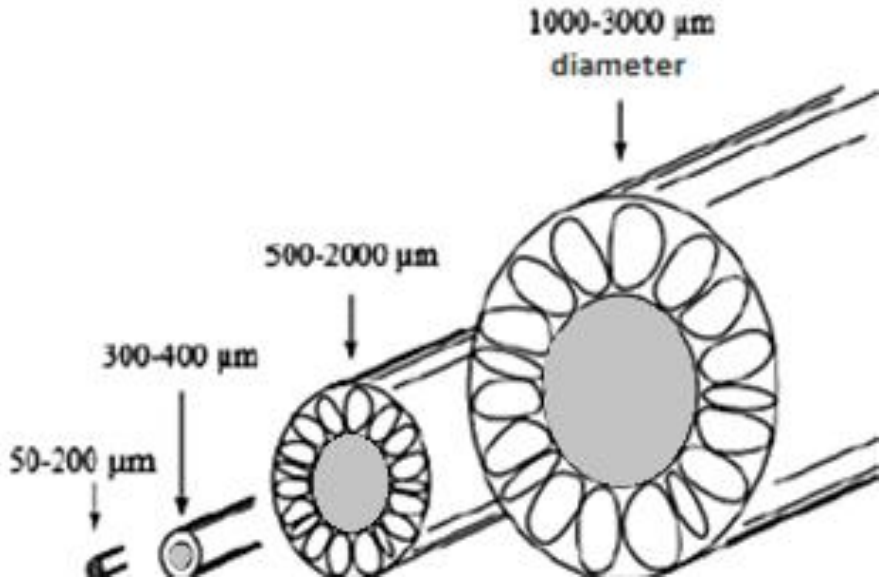

Figure 1.6 HF Membranes with Different Diameters [15]

1.2.3 Popular Membrane Materials

Materials for membranes are divided mainly into two groups as biological and synthetic membranes. Selective permeable membrane is used in many naturally occurring biological membrane processes such as the intake of water and vitamins in the soil by plant cells, the body skin protects the internal organs against microbial pathogens and prevents water loss, the transport of oxygen in the lung to the blood cells, and the filtration of urea in the blood by the kidney [12].

Also, synthetic membranes are divided into two groups as organic (polymeric) and inorganic (ceramic, metallic) [16]. High temperatures are usually preferred for industrial processes, therefore polymeric membranes are not suitable. Common polymers used in membranes are; cellulose acetate (CA), polysulfone (PS), polypropylene (PP), polycarbonates (PC), polytetrafluoroethylene (PTFE) and polyamide (PA), polyvinylene fluoride (PVDF) and common materials of inorganic membranes are zeolite, silicon nitride, silicon carbide, various oxides (aluminium, titanium, zirconium, silicon), steel, palladium, silver, and their alloys [1,17].

The first porous polymeric HF was used almost 60 years ago [18]. Since then, polymeric HF has used in gas separation and water treatment, and in the medical sector. Polymeric HF is produced at low cost by dry–wet spinning process [19, 20].

Polymeric membranes have higher porosity than other membranes and have easy functionality and they are cheaper and have more pressure stability and it can be produced easily than inorganic membranes [21].

Firstly, Mahon and et al. patented the method of preparation of permselective HF in Dupont in 1960s [22, 23]. Then, Dupont developed the polyethylene terephthalate (PET) HF for the recovery of light gases [24, 25]. Another application for gas separation is polysulfone HF developed by Monsanto [26, 27]. Cabbaso and et al. proposed the addition of polyvinylpyrrolidone (PVP) and this becomes common fabrication method of PS HF [28], it has good mechanical properties and easy-to-process for the spinning of HF [29-32]. PVDF has high mechanical strength, thermal stability, chemical resistance, and well-controlled porosity [33-35]. Zhang et al. used PVDF membranes to treat water containing bovine serum albumin [36]. It was found that the hybrid membranes offer excellent hydrophilicity, water permeability and

antifouling performance. Huang et al. prepared and characterized porous PTFE membranes [37]. CA HF has poor selectivity in the separation of gases [38]. Silicone rubber HF has low mechanical properties and selectivities [39]. Chung and et al. studied the effect of bore fluid chemistry on the morphology and performance of polyethersulfone (PES) HF for gas separation [40] and Chen and et al. fabricated PES HF for CO_2/N_2 separation [41].

However, polymeric membranes are susceptible to harsh condition like high temperature, pressure and chemical [42–44]. Polymeric HF has been used due to its high surface area per unit volume and high permselectivity [45–47]. The polymeric HF is limited to mild operating conditions due to its low thermal stability and ease of contamination [48]. It shows lower tolerance to abrasive particles, chemical cleaning, and steam sterilization procedures [49]. Therefore, a great deal of studies been conducted intensively to develop porous ceramic membrane.

Ceramic HF provides higher surface area to volume ratio, withstand cleaning approaches i.e. backwash, chemical treatment and has great mechanical strength so HF can be used in lots of applications [50]. Ceramic HF can be used at an ambient temperatures and high temperature applications [51, 52]. Ceramic HF has higher hydrophilicity than polymeric HF, and that makes water permeation without additional surface modification [53]. Also, the ceramic HF can be irradiated with UV light or a visible light to remove contaminations.

Su and et al. produced porous alumina ceramic membrane for reclaiming oil from oily water [54]. Okon et al. fabricated alumina nano-porous ceramic membrane for esterification application in petroleum refinery [55]. Alumina, zirconia and titanium HFs are expensive due to the materials are synthetic and have high melting point so that, they are limited for large-scale applications [56-58]. Therefore, low cost and green ceramic membrane from waste has great interest due to its availability. In 2014, Lu and et al. produced a porous mullite ceramic membrane from waste coal gangue (SiO_2 (70.08 wt%) and Al_2O_3 (17.36 wt%)) and bauxite to reduce the cost of manufacturing [59-61]. In 2016, Zhu and et al. fabricated ceramic HF membrane from waste coal fly ash (Al_2O_3 (44.76 wt%) and SiO_2 (44.17 wt%)) [62].

Inorganic membranes are more expensive than polymeric membranes but they have high operation temperatures, high mechanical stability, well-defined stable pore structure, and high resistance to solvent and corrosive chemicals [15].

The low fracture load and high brittleness properties of polymer and ceramic hollow fiber membranes are disadvantageous for industrial applications [63]. Metal based materials are used to solve these problems because they can provide high strength and toughness. Also, metallic materials have resistant to oxidative chemical and thermal cleaning treatments, and providing reusability properties [64]. Finally, welding or brazing processes are applied metallic membranes easily [63].

Austenitic 316L stainless steel (SS) is one of the most popular material in powder metallurgy (PM) [65]. Today, studies on stainless steel matrix composites have also started and gained considerable importance. Studies showed that mechanical properties of SS based HFs increase in stainless steel matrix composites. Distribution of the reinforcing element is important to obtain homogeneous properties. Among all ceramic based reinforcements, silicon carbide (SiC) is one of the most popular reinforcements. Aims of the reinforcing SiC element added to the matrix, is to improve the stiffness and thermal shock resistance of HF's [66].

In terms of reinforcement, SiC and TiC are the most favourable ones. Patankar et. al. studied the behaviour of TiC, SiC and 316L SS powder during sintering process [67]. TiC/316L is sintered at 1300 ºC and SiC/316L is sintered at 1200 ºC, and addition of SiC improved elongation, while TiC addition lowered ductility [68].

There are different articles about particle size importance in HF [69]. There are different studies about the small or mixed particles sizes are better in HF's. Particle size effects compressibility, therefore densification and mechanical properties of the sintered products increase [70]. It means that higher density of 316L samples improve the mechanical properties [65].

There are few studies about metallic hollow fiber membranes in the literature, and it has gained importance in recent years and the number of studies has increased. Luiten-Olieman et al. produced porous stainless steel (SS) hollow fiber membranes in 2011 by dry-wet spinning technique and obtained high strength and high gas permeability [71].

SS hollow fibers are produced with high bending strength and CO_2 and N_2 permeability by using 6 micron particle size stainless steel powder and poly etherimide (PEI) binder in study of Schmeda-Lopez et al. [72, 73].

Also, Michielsen et al. produced SS HF membranes by robotic fiber deposition method and reported that the microstructure consisted of a sponge-like structure without large pores [74]. In 2017, Chong et al. investigated SS-ceramic composite hollow fibers and examined microfiltration properties. Aim of the study was filling the large pores with small particles to obtain small pores and as a result, the pore size was reduced to very small values [75]. Also in 2017, Allioux et al. produced porous HF membranes with two different particle size stainless steel powders. As a result, densification and water permeability were increased [76]. Consequently, results of studies show that metallic HF membranes are more advantageous than other materials [77].

1.2.4 Spinning Methods

Hollow fiber membrane structures are divided into two groups as symmetrical and asymmetrical. There are two structures as upper and lower layers in asymmetric membrane structure. The top is a selectively permeable layer that has less-porous or dense structure. The lower layer is the support layer that increases the mechanical resistance [78].

Spinneret is used to give the fibers their hollow shape. The first patent for the spinneret on behalf of Dow chemical company was taken by Mahon [79]. This part, also known as a nozzle, consists of small channels and a capillary tube in an outer orifice. Before membrane production, this part should be cleaned with solvent and maintained regularly. The function of the nozzle is to direct the mixture and determine the membrane inner diameter. Figure 1.7 shows the structure of hollow fiber membrane.

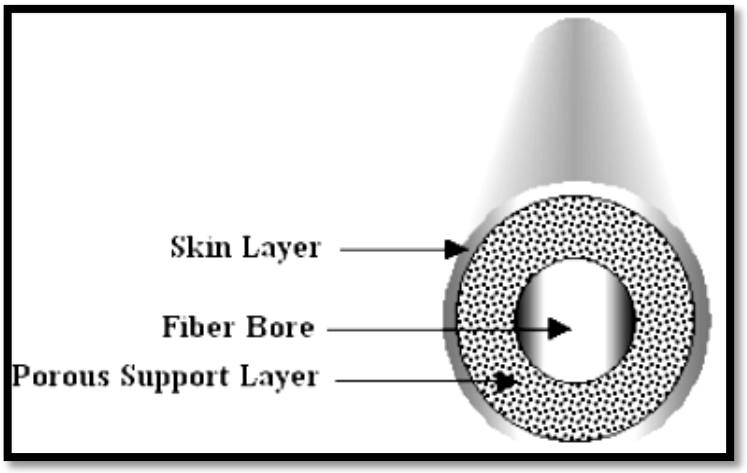

Figure 1.7 A Schematic Structure of HF Membrane

Hollow fiber membranes have various production methods [80]. The first method is the "Melt Spinning". In this method, the polymer is heated and melted to form fiber. Melted polymer is pumped into the nozzle as a viscous liquid. The fibers formed are solidified by cooling and the solvent is not evaporated. The second method is the "Solution Spinning Process". Additional steps are required for the fiber to solidify so it is more complex than the melt spinning process. Solution spinning process is based on the phase inversion technique and is divided into three groups as dry spinning, wet spinning and dry-wet spinning [81]. The dry spinning process begins with dissolving the polymer in an organic solvent. This viscous solution passes through the nozzle as filaments, and the process ends when the fibers solidify. In the wet spinning process, the nozzle is placed in coagulant bath containing a liquid that is miscible with the solvent in the polymer solution but cannot dissolve the polymer. During spinning, the polymer solution passes from the nozzle to the bath and the polymer forms to solid fibers [82].

In the most popular "dry-wet spinning" process which is used in this thesis and as shown in Figure 1.8, a polymeric viscous fluid solution called spinning solution is formed [83]. This solution is pumped through the nozzle outer orifice. Then, water is pumped from the centre of the nozzle as a coagulant to create the inner space. After the polymer solution leaves the nozzle through the air gap, it enters an external coagulant and phase inversion occurs. In other words, the liquid polymer solution

turns into solid-state hollow fiber membranes. The distance of the nozzle equipment from the coagulant bath affects the outer wall thickness of the membrane [84].

During the spinning process, exchange of solvent and non-solvent makes thermodynamic instability of the mixture and cause phase separation into a polymer lean phase (liquid phase that forms the pores) and polymer rich phase (solid phase that forms the membrane structure) [85]. This is called as phase inversion method. The solvent evaporates in coagulation bath, the polymer rich phase solidifies, at the same time, and catch the SS particles [86]. Heat treatment eliminates the polymer and sinters the SS particles [87].

Phase inversion occurs at two points: slow phase inversion at the interface between the polymer solution and the internal coagulant fluid, and faster phase inversion at the interface between the polymer solution and the non-solvent bath. The fiber produced is then dried before being heat treated. These phase inversion processes allow the formation of asymmetric membrane structures [88].

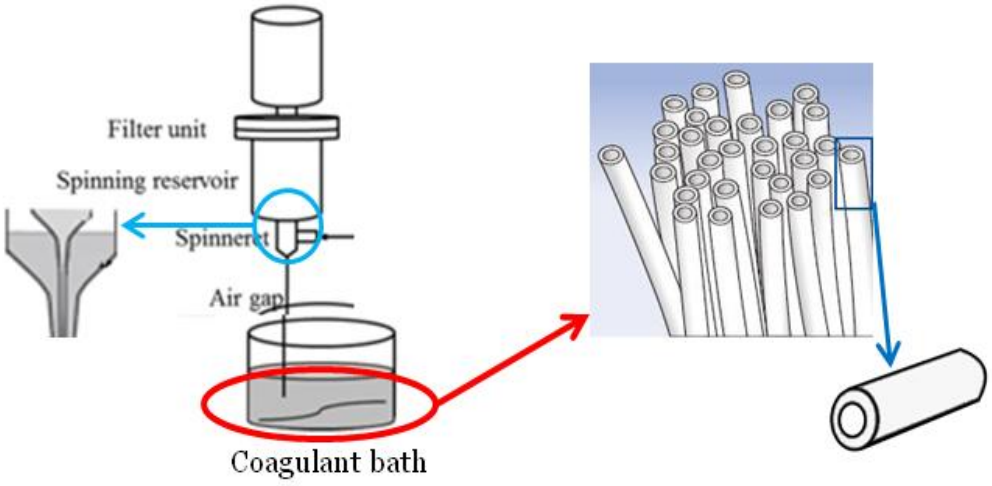

Figure 1.8 Schematic Representations for the Spinning Process

PVP (polyvinylprolidone) is added to the polymer solution as a secondary polymer is used to create pores. An environment consisting of PVP is formed in the pore walls (between pores and polymers). PVP easily passes into water so it can be easily removed by drying and post-production processes [89].

The composition (solvent, additive) of the polymer solution, the duration of a dry phase inversion, air moisture, spinneret distance (air gap), dope viscosity, dope extrusion rate, the temperature of the polymer solution and the coagulation bath are important parameters for hollow fiber membranes [90].

1.2.5 Sintering Mechanism

Sintering is a heat treatment method that creates and joins the intergranular bond of powder particles by temperature lower than the melting point, as shown in Figure 1.9. Sintering solidifies the materials depending on external factors such as grain size, temperature and time. Also, necking occurs between the particles in contact which increases the materials strength [91]. Sintering step on green hollow fibers is important to remove organic additives and binders [92].

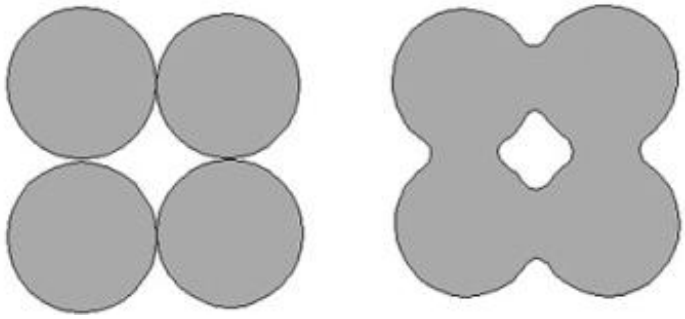

Figure 1.9 The Common Sintering Principle [93]

Sintering atmosphere is very important in PM process [94]. Figure 1.10 shows the sintering steps. Hydrogen, nitrogen or argon atmospheres are used to protect stainless steel (SS) hollow fibers during the sintering process [95, 96]. The sintering atmosphere effects the mechanical properties and corrosion behaviours of HF membranes [97]. Rui et al. studied the effect of sintering atmosphere in the production of 316l stainless steel hollow fiber membranes by dry-wet spinning technique [95]. Nitrogen atmosphere gives higher flexural strength and Argon or hydrogen atmospheres give better flexibility and corrosion resistance [94].

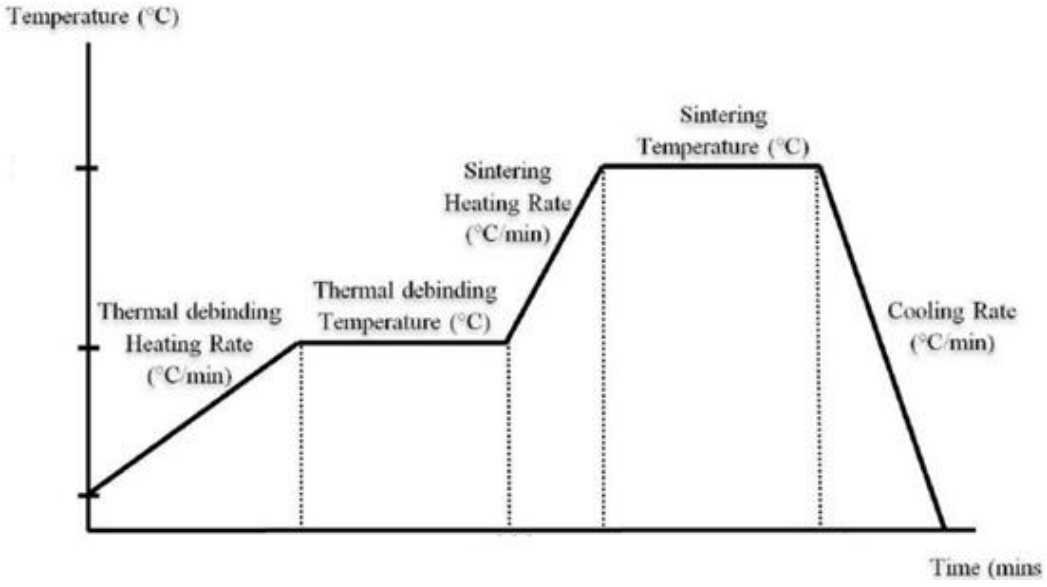

Figure 1.10 Heating Regime for the Sintering [98]

Also, high sintering temperature is preferred to achieve higher sintered density and less surface oxides. Reduction of surface oxides leads to increase corrosion resistance and ductility [99]. Also, oxygen, carbon, nitrogen and iron contamination determine corrosion behaviours of membranes [100]. Sintering of SS in nitrogen atmospheres results in precipitation of chromium nitride, and it leads to advanced mechanical properties but degradation of corrosion resistance [99]. Moreover, increasing carbon and nitrogen content increase strength and hardness, but reduces ductility [101].

Sintering has two main types as conventional sintering methods and fast sintering methods. In the conventional sintering, temperature, time and atmosphere can be adjusted. In addition, it enables the heat treatment of the part after sintering by removing additions such as lubricant and binder.

Conventional sintering furnaces are divided into two groups as batch sintering which is serial sintering method and continuous sintering that samples are sintered on a moving belt [102].

Fast sintering techniques include induction sintering which occurs as a result of heat generation by the current induced into powder metal samples in a magnetic field, spark plasma sintering, direct electric current pass through the powder sample inside

the graphite mold [103, 104], laser sintering that powder sample sintered layer by layer for 3D part manufacturing and SLM and SLS methods belong to this group [105, 106] and microwave sintering, electromagnetic energy interact directly to the sample.

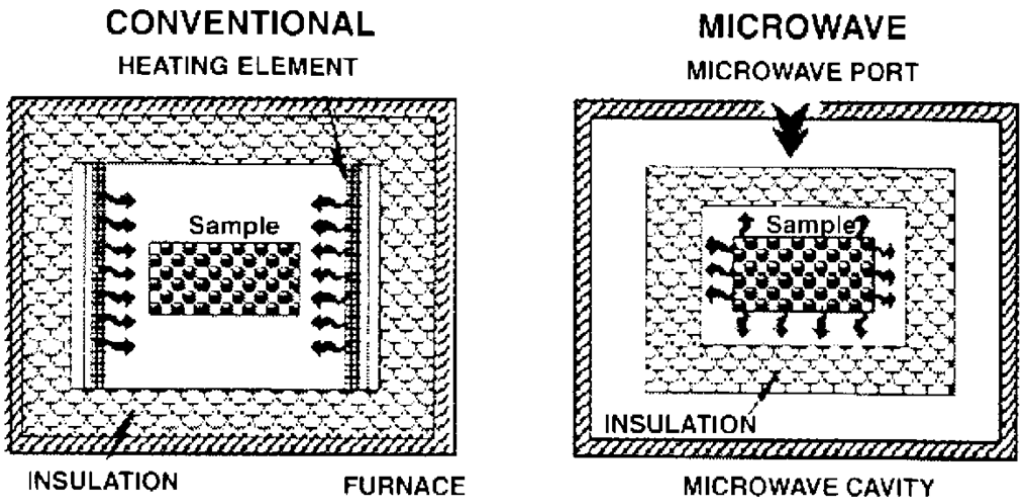

Figure 1.11 Working Principles of Microwave and Conventional Sintering Furnaces [107]

In sintering process, sample made from powder particles is heated from room temperature to the lubricant melts and vaporizes temperature, then heated to sintering temperature and held for a specific time. High heating rate makes distortion and inhomogeneous microstructure. Therefore, slower heating rate is preferred to prevent thermal gradient but it increases the operation time, cost and grain coarsening [108].

In this method, electrical energy converted into heat energy is transmitted to the material surface through radiation and convection. It is then transferred to the interior of the material via transmission. As a result, the surface of the sample is at higher temperature, while its interiors are at lower temperatures. Difference between conventional and microwave sintering furnace is shown in Figure 1.11.

1.2.6 Gas Permeability Process

Gas separation is the separation of gas components. It is carried out based on the concentration and pressure difference between two media such as gas-gas. Both porous and dense membranes are used as gas separation barriers.

If the pores are larger than 0.1-10 μm, the gases are filtered by convective flow which is transport of fluid across a porous membrane driven by the applied pressure and no separation occurs. Movement through the pores is called as Knudsen diffusion. Gas molecules interact with the fiber walls and low molecular weight gases diffuse faster so separation occurs in Knudsen diffusion [109]. As the gas size decreases, both the permeability and the solubility of the gas increase. Figure 1.12 represents the gas separation process.

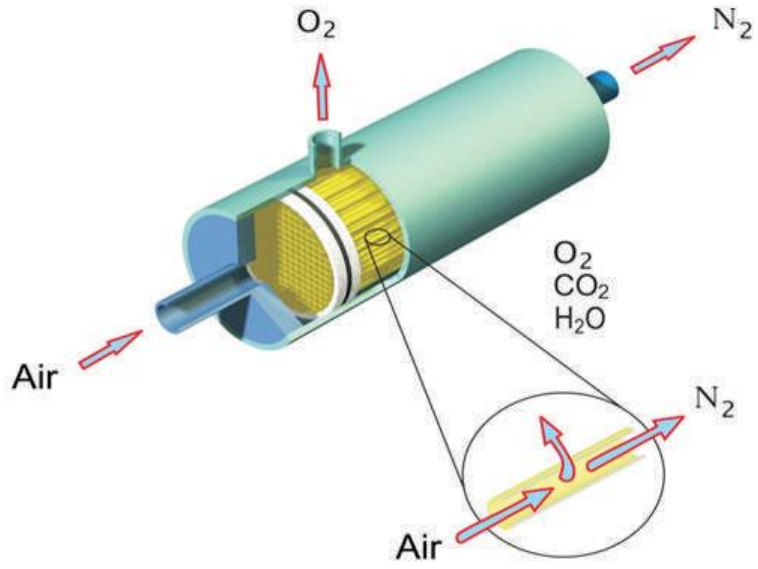

Figure 1.12 Separation Mechanism for N_2 and O_2 Gases [110]

The gas permeation mechanism in dense membranes is known as solution diffusion. While there is high flux and low selectivity for gas separation with porous membranes, non-porous membranes have low flux and high selectivity [86].

1.3 Literature Overview

Table 1.1 Studies About Production of Hollow Fiber Membranes [4].

RESEARCHER	ARTICLE NAME	MIXTURE	METHOD
Ming Wang, Ming-Ling Huang, Yue Cao, Xiao-Hua Ma, Zhen-Liang Xu	Fabrication, separation and characterization properties of three-channel stainless steel hollow fiber membrane [Journal of membrane science (2016)]	*316L (9.4 μm) *NMP *PES *PVP	DRY-WET SPINNING PROCESS
JooWon Oh, Seung Kyu Ryu, Won Sik Lee, Seong Jin Park	Analysis of compaction and sintering behaviour of 316L stainless steel nano/micro bimodal powder [Powder Technology (2017)]	*316L (4 μm) *316L (100 nm)	MIXTURE OF TWO DIFFERENT SIZED POWDERS
Wenjie Rui, Chun Zhang, Chao Cai, Xuehong Gu	Effects of sintering atmospheres on properties of stainless steel porous hollow fiber membranes [Journal of membrane science (2015)]	*316L (8 μm) *PESf *NMP *DEONISED WATER	DRY-WET SPINNING PROCESS
Jeng Yi Chong, Bo Wang, Kang Li	High performance stainless steel-ceramic composite hollow fibres for Microfiltration [Journal of membrane science (2017)]	*316L (3 μm) *YTTRIA STABILIZED ZIRCONIA NANOPART. (30-60 nm) *NMP *PMMA *ARLACEL P135	DRY-WET SPINNING PROCESS

Table 1.1 (continue.) Studies About Production of Hollow Fiber Membranes [4].

RESEARCHER	ARTICLE NAME	MIXTURE	METHOD
Mieke W.J. Luiten Olieman, Louis Winnubst, Arian Nijmeijer, Matthias Wessling, Nieck E. Benes	Porous stainless steel hollow fiber membranes via dry–wet spinning [Journal of membrane science (2011)]	*316L (4 μm) *NMP *PES *PVP *DEONISED WATER	DRY-WET SPINNING PROCESS
Diego R. Schmeda-Lopez, Simon Smart, Eduardo H.M. Nunes, Daniela Vasconcelos, Wander L. Vasconcelos, Martin Bram, Wilhelm A. Meulenberg, João C. Diniz da Costa	Stainless steel hollow fibres – Sintering, morphology and mechanical Properties [Separation and Purification Technology (2015)]	*316L (6 μm) *316L (10 μm) *316L (16 μm) *NMP *PEI *PVP	DRY-WET SPINNING PROCESS
Francois-Marie Allioux, Oana David, Miren Etxeberria Benavides, Lingxue Kong, David Alfredo Pacheco, Tanaka Dumée, Ludovic F. Dumée	Preparation of Porous Stainless Steel Hollow Fibers through Multi-Modal Particle Size Sintering towards Pore Engineering [Membranes MDPI (2017)]	*316L (10 μm) *316L (20 μm) *316L (44 μm) *NMP *PES	DRY-WET SPINNING PROCESS
Diego R. Schmeda-Lopez, Simon Smart, Wilhelm A. Meulenberg, João C. Diniz da Costa	Mixed matrix carbon stainless steel (MMCSS) hollow fibres for gas separation [Separation and Purification Technology (2016)]	*316L (6 μm) *316L (10 μm) *316L (16 μm) *NMP *PEI *PVP	DRY-WET SPINNING PROCESS

Table 1.1 (continue.) Studies About Production of Hollow Fiber Membranes [4].

RESEARCHER	ARTICLE NAME	MIXTURE	METHOD
Ming Wang, Qi-feng Zhong, Zhen-Liang Xu, Xiao-hua Ma	Modification of porous stainless steel hollow fibers by adding TiO2, ZrO2 and SiO2 nano particles [Journal of Porous Materials (2016)]	*316L (25 μm) *TiO_2 (300 nm) *SiO_2 (300 nm) *ZrO_2 (300 nm) *DMAc (solvent) *PAN (binder) *PVP (viscosity en.)	DRY-WET SPINNING PROCESS

Joo Won Oh and et al. used nano powders due to its advantages, such as more isotropic shrinkage, better surface and green strength. Since the surface area increases surface energy, nano powder has low sintering temperature with low activation energy [111, 112]. However, larger surface area causes agglomeration and decrease packing density. Therefore, nano/micro bimodal powder samples give better mechanical properties. As a result of study, 25:75 bimodal powder gave highest relative density.

Wenjie Rui and et al. aimed to reveal the effect of sintering atmospheres on the properties of HF's. The air and CO_2 atmospheres cause metal oxidation and decrease mechanical strength of HF. The inert atmospheres (N_2 and He) avoid metal oxidation but carbon remains in the SS HF so the corrosion resistance to water decreases. As a result of the study, H_2 is effective to remove additives from HF. Also, it gives higher bending strength and toughness. Finally, as a result of study, 1050 ºC and 1100 ºC are found as appropriate sintering temperature.

Jeng Yi Chong and et al. produced dual-layer SS/SSYSZ hollow fibres. The outer layer was a mixture of SS and YSZ (30-60 nm). YSZ filled up the pores between the SS particles and decrease the pore size of HF as shown in Figure 1.13. As a result of study, this geometry increased the fracture load of HF. The dual-layer hollow fibres also demonstrated excellent mechanical properties compared to ceramic hollow fibres.

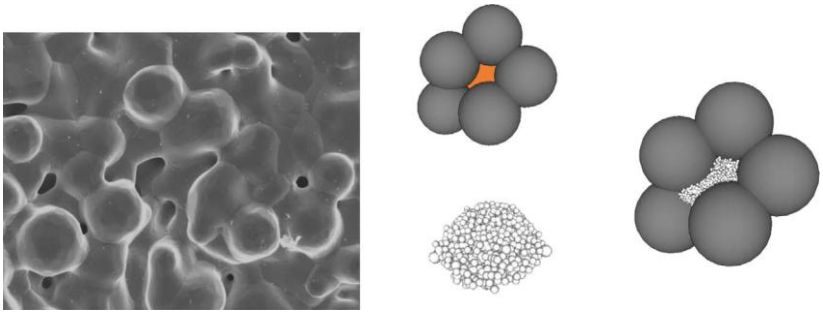

Figure 1.13 Image of Filling Pores Between the SS Particles [113]

Mieke W.J. Luiten Olieman and et al. studied about sintering temperature of SS HF samples. The temperature bigger than 1100 ºC decreased the nitrogen permeability and increased the bending strength of HF because of the densification. When SS HF sintered at 1050 – 1100 ºC, the strength and nitrogen permeability results were better as compared to ceramic counterparts.

Diego R. Schmeda-Lopez and et al. investigate the effects of sintering conditions on SS HF with particle size. As a result of study, smaller particles give more sponge-like region so it produced mechanically stronger hollow fibres. However, large particles have limited mass transfer transport rate and neck formation. Therefore, it produces finger like and macrovoids which gives weak mechanical properties.

As a results of study, small particles (6 and 10 µm), sintering between 1050 ºC and 1100 ºC at 1 - 4 hours at argon or nitrogen atmospheres give better mechanical strengths.

Francois-Marie Allioux and et al. fabricated the HF's by mixing different sizes SS particles. As a result of study, the sintered HFs from particles of two different sizes showed more stable mechanical properties. In addition, the sintered mix of 10 - 44 µm particle size hollow fibers showed smaller average pore size (<1µm) as compared to 10 µm and mix of 10 - 20 µm particle size.

Diego R. Schmeda-Lopez and et al. produced a mixed matrix carbon stainless steel (MMCSS) hollow fibres. As a result of study, mixing different particle size gave denser structure so the mechanical properties of HF increased when SS particle size decreased.

Ming Wang and et al. used 316L SS particle size of 25 μm and TiO_2 particle size of 300 nm, SiO_2 particle size of 300 nm, and ZrO_2 300 nm particle size to produce HF. As a result of study, the mechanical strength increased after the adding of TiO_2 nano-particles in the HF.

Based on these studies, it was foreseen that small particles and composite structure would give the best structure and mechanical properties. Therefore, mix of different particles, and composites were used in this thesis.

2. MATERIALS AND METHODS

2.1 Materials and Chemicals

In this study, 3µm (fine) and 20-53µm (coarse) 316L stainless steel powders (obtained by Sigma Aldrich and Höganas-AB, respectively) are used as the matrix powder and SiC powder having average particle size (APS) of 8 µm is used as reinforcement, as shown in Figure 2.1 and Figure 2.2. Also, polymethylmethacrylate (PMMA), N-Methyl-2-pyrrolidone (NMP), and polyvinylpyrrolidone (PVP), obtained by Sigma Aldrich, are used as polymeric binder, solvent and viscosity adjusting materials respectively. The chemicals are not pre-treated.

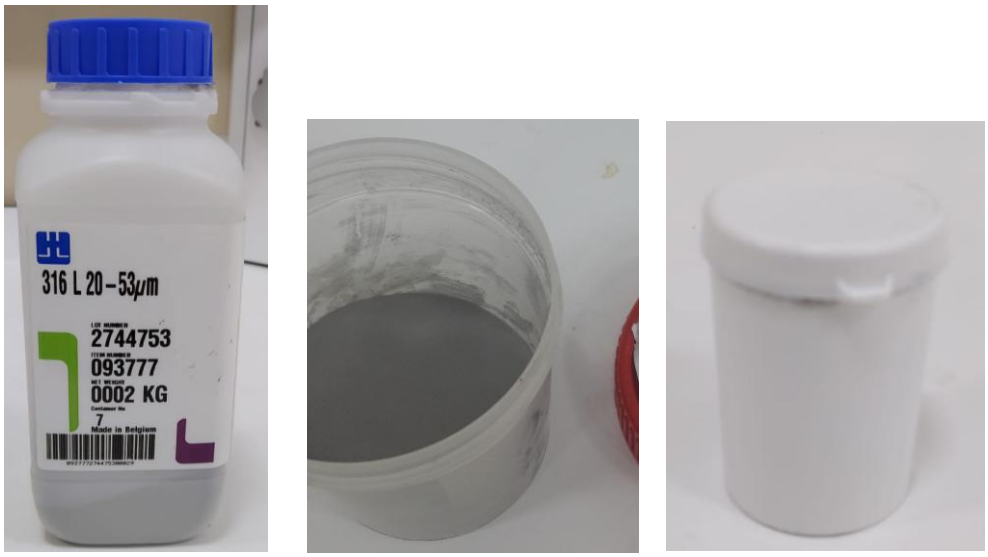

a b c

Figure 2.1 a) Coarse 316L SS, b) Fine 316L SS, c) SiC Powder

a b c

Figure 2.2 a) NMP, b) PMMA, c) PVP

2.2 Solution Preparation Procedure

The solid loading of 70 wt% was chosen as this content would give the optimum properties [114]. The solution preparation step starts with the mixing of PMMA and NMP for 12 hours. Then, 316L SS powders are added to solution slowly and are mixed for 3 hours. Also, composite powder mixture (95%wt. 316L + 5%wt. SiC) are added to the another PMMA-NMP solution slowly and mixed for 3 hours. Finally, PVP is added and all of them are mixed for 30 mins. This suspension is then placed in a vessel and the vacuum is degassed. After degassing, the spinning suspension pressure is increased with the help of syringe pump and extrusion is performed with the help of spinneret. The amounts of components in the solution are given in Table 2.1 and solution preparation devices are shown in Figure 2.3.

Table 2.1 Mass Values of Components in the Solution.

	316L	**NMP**	**PMMA**	**PVP**	**SiC (5%wt.)**
Stainless Steel Suspension Composition	42 g	14.4 g	4.2 g	0.2 g	-
Composite Suspension Composition	39.9 g	14.4 g	4.2 g	0.2 g	2.1 g

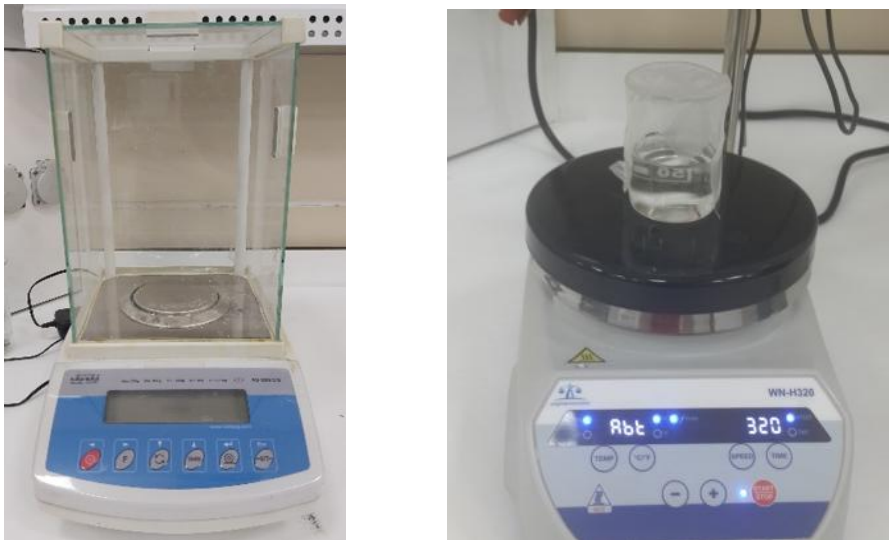

a b

Figure 2.3 Solution Preparation Devices; a) Analytical Balance, b) Magnetic Stirrer

Six different compositions were prepared for this thesis and representative codings are shown in Table 2.2. These are respectively; 20-45 (coarse) micron powder, 3 (fine) micron powder, 20-45 micron powder + 3 micron powder, 20-45 micron powder + SiC, 3 micron powder + SiC, and 20-45 micron powder + 3 micron powder + SiC.

Table 2.2 Six different compositions.

Sample Codes	Compositions (wt%)
1) C-SS	100% coarse 316L powder
2) F-SS	100% fine 316L powder
3) M-SS	mixed (75% fine+25% coarse) 316L powder
4) C-COMP	coarse 316L + 5% SiC
5) F- COMP	fine 316L+ 5% SiC
6) M-COMP	mixed 316L powder + 5% SiC

2.3 Production Procedure

Hollow fiber membranes are produced by the dry-wet spinning technique. Membrane production setup consists of pressure source, solutions, pumps, nozzle, internal coagulant and coagulation bath. The main parts of the extrusion setup used in the production of fibers are shown in Figure 2.4.

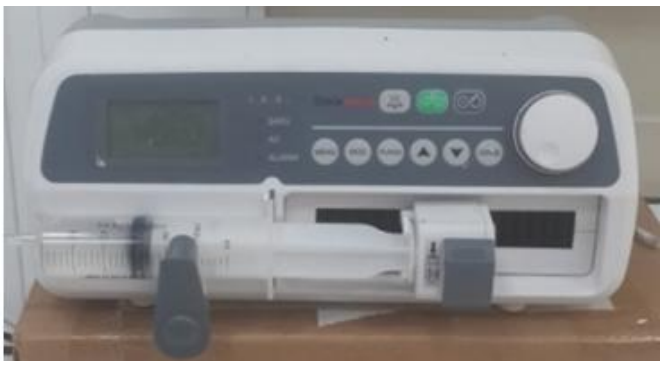

a

b

Figure 2.4 Main Parts of Production Setup, a) Syringe Pump, b) Nozzle

The solution and the internal coagulant are simultaneously pumped towards the nozzle, as shown in Figure 2.5. They are flow through the coagulation bath after passing through the air gap at definite distances. The HF samples were kept in pure

water in a bath for 1 day to remove from solvent and additives, and solidification is provided. Then they are taken from the bath to dry for 1 more day and kept on a paper. Finally, the green samples become ready for the sintering stage.

Figure 2.5 Photo of the Nozzle System

2.4 Sintering Processes

After production process, sintering stage begins in order to increase the strength of HF's without any deterioration of their structure. After these processes, no final treatment was applied to hollow fiber membranes.

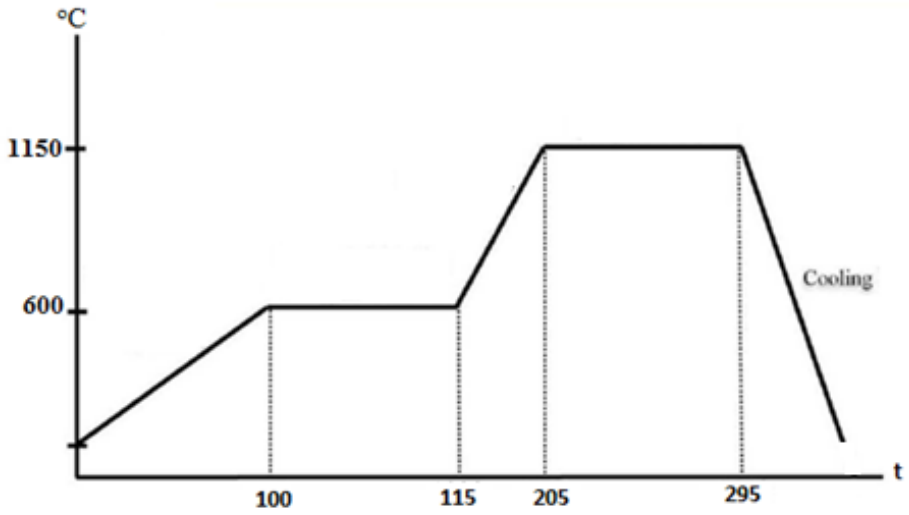

Figure 2.6 Sintering Cycle of the Process

Two different sintering atmospheres are used in this thesis. These are argon gas and nitrogen-hydrogen gas mixture. Hollow fiber green bodies is sintered in two different gas mixture (90% N_2/10% H_2 and 100% Ar) in temperatures of 1150^oC for 90 mins as shown in Figure 2.6.

Figure 2.7 Tubular Sintering Furnace

Figure 2.7shows conventional sintering furnace and Figure 2.8 shows the produced of hollow fiber membrane samples sets. All this process is called dry-wet spinning technique in the literature. Thus, microstructure, mechanical and gas permeability properties for two different sintering methods will be examined separately.

Figure 2.8 Image of the Produced HF Samples Sets

2.5 Characterization Studies

The effects of sintering atmospheres, different particle size and different compositions on samples are characterized to obtain chemical compositions, electrical resistivity, pore amount, average pore size and pore shape and distribution. The hollow fibers are then subjected to a 3-point bending test to determine their mechanical properties. Finally, the gas permeability is examined with nitrogen (N2) permeability test.

2.5.1 Scanning Electron Microscope and EDX Analysis

Hitachi TM3030 Plus and Zeiss Sigma 300 VP SEM devices were used to obtain cross-sections, inner and outer surface views of the membranes produced and to reveal membrane morphology, as shown in Figure 2.9.

a b

Figure 2.9 SEM Devices Used in the Study, a) Zeiss Brand and b) Hitachi Brand

2.5.2 X-Ray Diffraction Analysis

The crystal phases of SS hollow fiber membranes were determined by Bruker D2 Phaser device which is shown in Figure 2.10.

Figure 2.10 Image of X-Ray Machine

2.5.3 Electrical Resistivity Analysis

The electrical resistance of the stainless steel hollow fiber is measured with a multimeter (Keysight, 34461A Digit Multimeter) as shown in Figure 2.11.

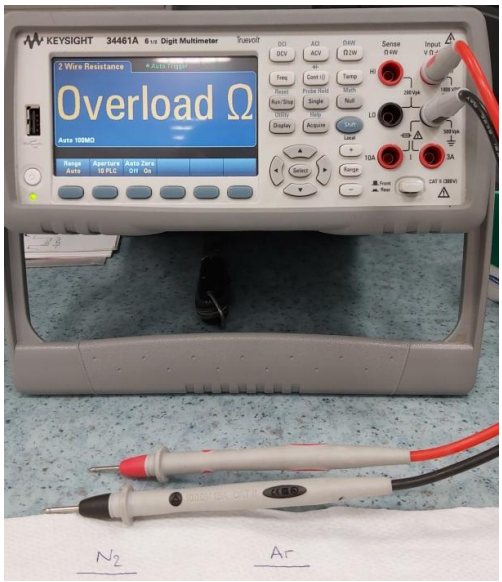

Figure 2.11 The Multimeter Used in the Study

2.5.4 Mercury Porosimetry Analysis

The pore size distribution is measured with a mercury porosimetry analyzer (AutoPore IV 9500, Micromeritics Instrument Corporation) as shown in Figure 2.12.

Figure 2.12 The Mercury Porosimeter Analyzer Used In Study

2.5.5 Bending Test

3-point bending test is used to determine the mechanical properties of samples by using universal Shimadzu AG-IC material testing machine shown in Figure 2.13.

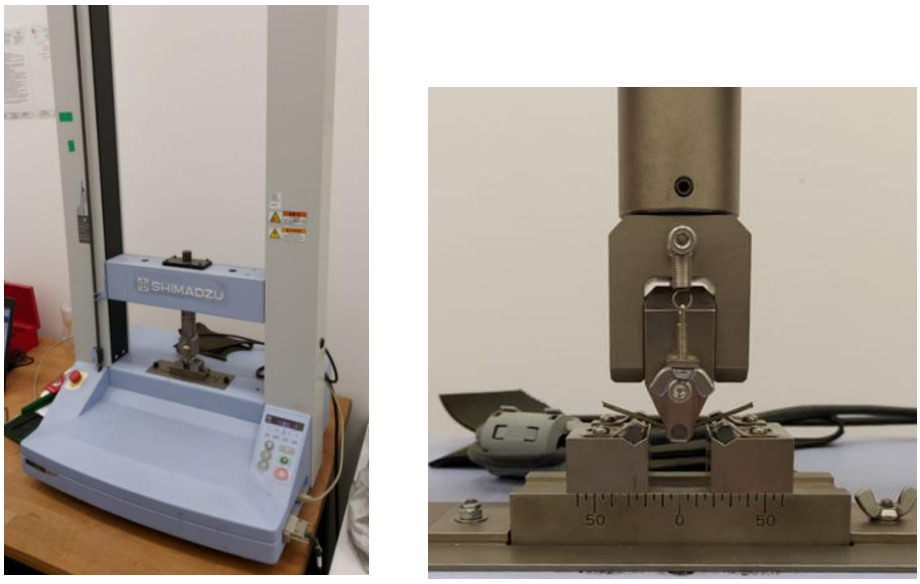

Figure 2.13 3-Point Bending Test Machine (Shimadzu AG, Japan)

The bending strength was (σ_f) was calculated from the equation below [92, 115]:

$$\sigma f = \frac{8FLD}{\pi(D^4 - d^4)} \quad (2.1)$$

where F is the fracture force (N), L is the length, D is the outer diameter and d is the inner diameters of the HF samples (m).

In this thesis, samples in 26 mm length, 1.70 mm as outer diameter and 1.10 mm as inner diameter are used.

2.5.6 Gas Permeability Test

Pure N_2 gas were used and tested at room temperature with operating pressures of 3 bars. The image of samples and setup scheme are shown in Figure 2.14 and Figure 2.15 respectively. A pressure gauge was connected to HFs and permeability rate were calculated by a formula. Permanence of HF was calculated by the following equations [63];

$$\left(\frac{Pi}{l}\right) = \frac{Qi}{(Ax\Delta P)} = \frac{Qi}{(n\pi \mathrm{D} x \Delta P)} \quad (2.2)$$

Where (Pi/l) is the gas permanence of a membrane, i is the gas species penetrate to the membrane, Qi is the volumetric flow rate of gas i at standard temperature and pressure (cm^3s^{-1}), A is membrane surface are (cm^2), ΔP is the pressure difference between the feed side and permeation side of the membrane (cmHg), n is the number of fiber in module, D is the outer diameter of the HF (cm), and l is the effective length of the HF.

The ideal selectivity of gas I and j is given by equation;

$$\alpha \mathrm{i/j} = \left(\frac{Pi}{\mathrm{L}}\right)\left(\frac{Pj}{\mathrm{L}}\right) \quad (2.3)$$

i/j is the selectivity of species gas i to species gas j, Pi/L and Pj/L are the permanence of gas I and j, respectively.

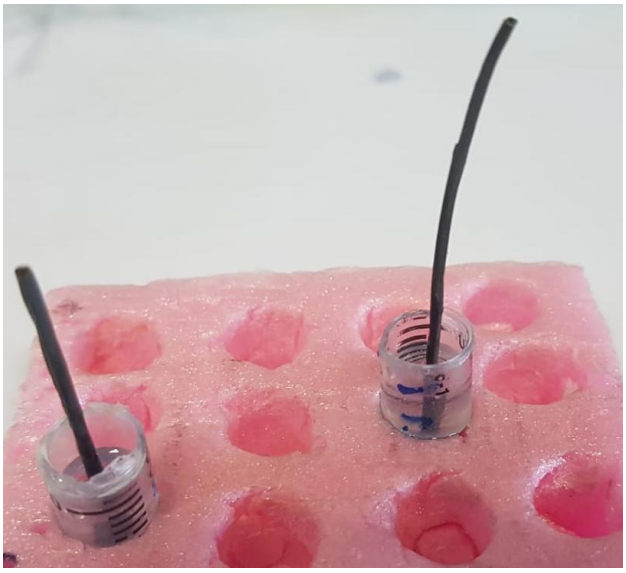

Figure 2.14 Image of Hollow Fibers and Epoxy Mold

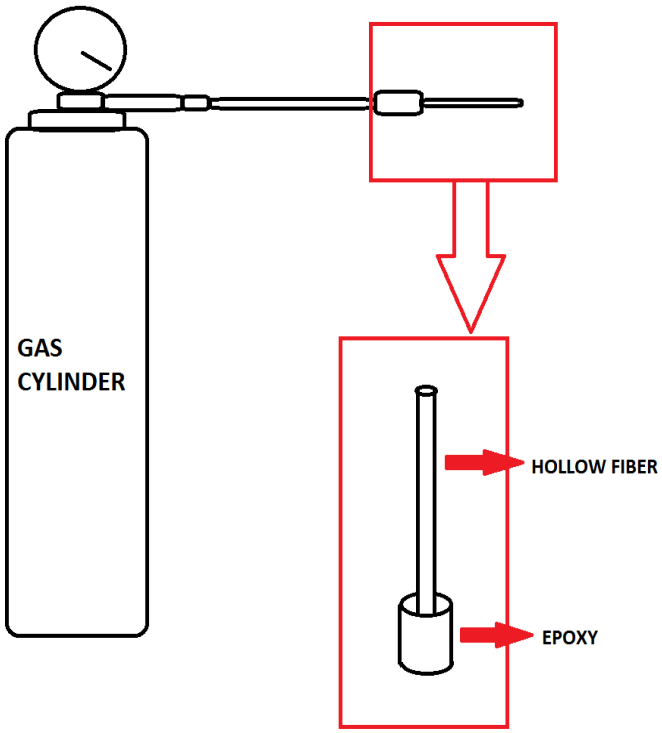

Figure 2.15 Scheme of Gas Permeability Test Setup

3. RESULTS AND DISCUSSION

3.1 Unsintered Samples

Figure 3.1 represents the SEM images of the unsintered 316L and composite HF samples. Samples made of coarse particles have inhomogeneous cross sections, and contain very large pores in the center of the HF as seen in A1-3 and D1-3. Samples made of fine powders have homogeneous cross sections as similar with many literature studies (B1-3 and E1-3) [71, 72, 116].

The asymmetric structures containing both sponge-like regions and finger-like voids are shown in B1.2, C1.2, E1.2 and F1.2 images. Also, large pores (voids) are obvious (see A1.2, B1.1, C1.3, and F1.2) parallel with the similar composite study in the literature [72]. However, these large dark areas have the potential of inhibiting effective sintering.

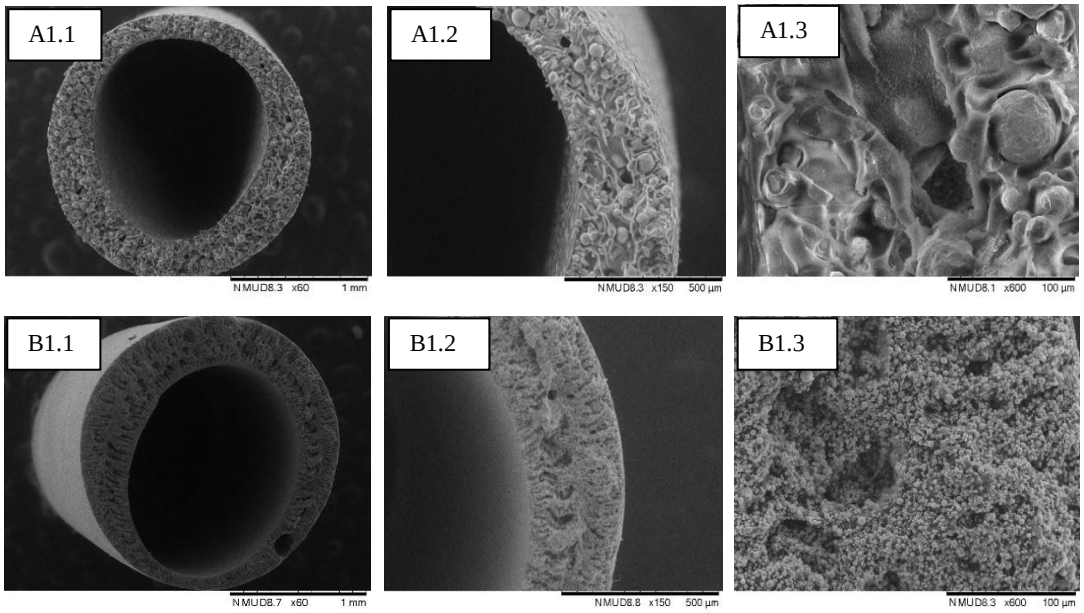

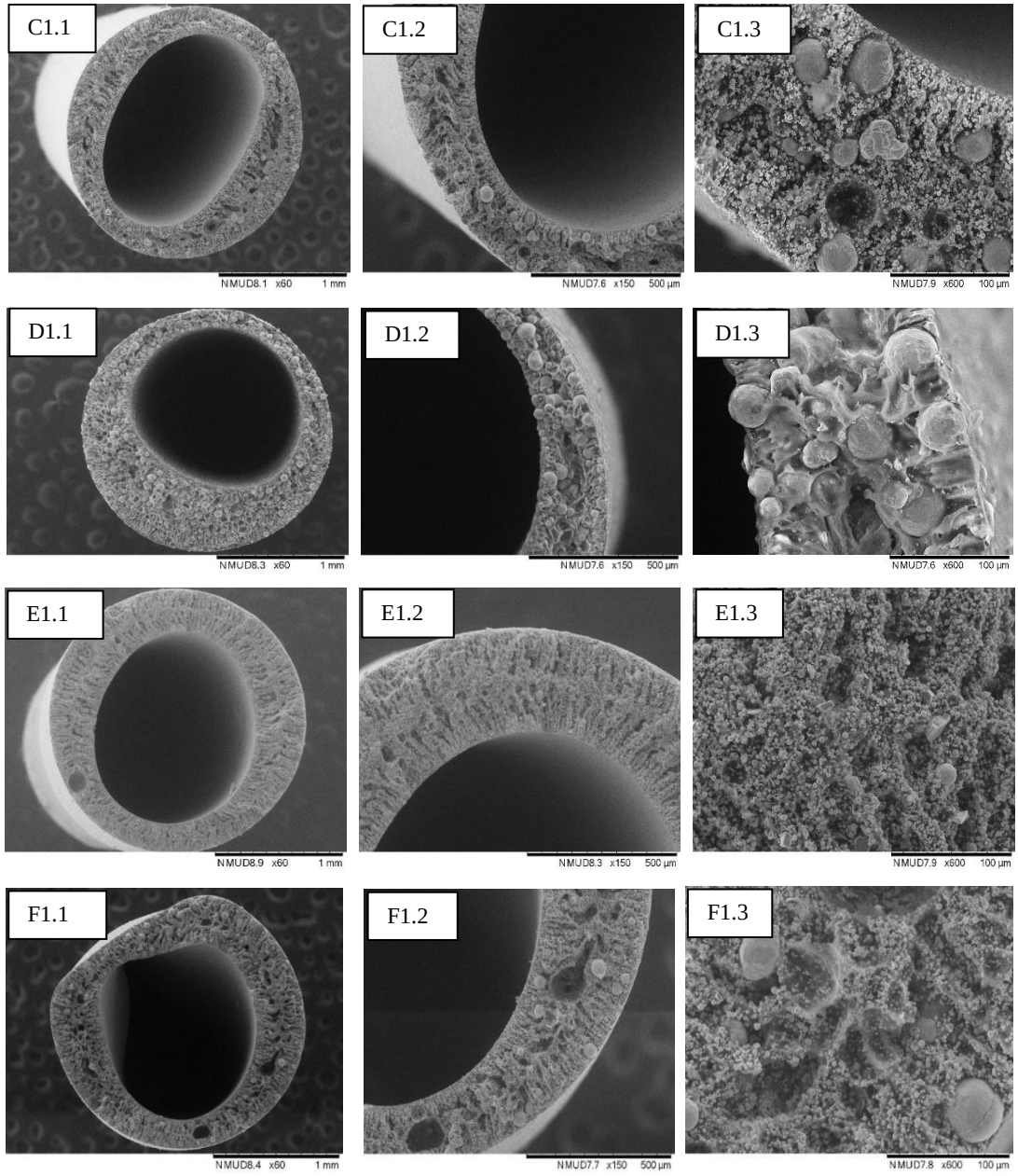

Figure 3.1 Three Different Magnificant Belong to Unsintered Samples A1.1-1.3) C-SS, B1.1-1.3) F-SS, C1.1-1.3) M-SS, D1.1-1.3) C-COMP, E1.1-1.3) F-COMP, F1.1-1.3) M-COMP

3.2 Sintered 316L Samples

Figure 3.2 shows the images of unsintered and sintered 316L SS samples.

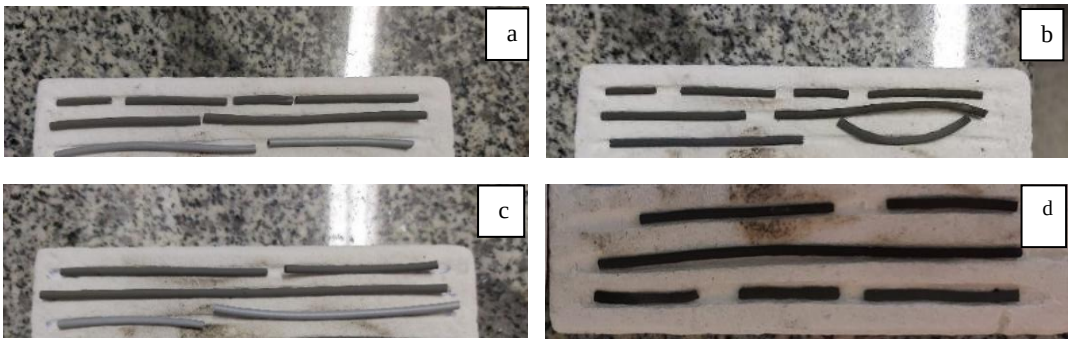

Figure 3.2 316L SS Samples, a) Unsintered, b) Sintered in N_2/H_2 Atmosphere, c) Unsintered, d) Sintered in Ar atmosphere

3.2.1 Scanning Electron Microscope and EDX Analysis

SEM images were used to evaluate the morphology of the fibers. Figure 3.3 shows the SEM images of the cross-sections of N_2/H_2 sintered 316L samples. Both spinning and sintering processes were performed successfully as shown in Figure 3.3. It can be clearly seen that HF samples have homogeneous hollow structure and shape.

For the sintering applied in nitrogen-hydrogen atmosphere which has a potential of preventing from oxidation as well as some amount of chromium nitride formation, it seems all the polymeric binder pyrolysed from HF structure. When particle sizes are compared, membrane with finest particles has higher densification in terms of microstructure, also have a dominant finger-like structure but also some sponge-like structures. These two structures are typicall which are the required signs from hollow fibers. The finger-like structure occurs from inner surface, the sponge-like structures are located at the outer region of the cross-section [73]. The finger-like voids were generated due to fast exchange between solvent (NMP) and no-solvent (water) while sponge-like structure was formed due to slow exchange during the spinning process [117].

Sponge like structures and finger like voids become dominant for the fine particle size HFs (F-SS). The finger-like structures are observed in B2.1 while sponge-like structures are observed for C2.1. For the samples with coarse particles A2.1-A2.3,

large pores are obtained. Therefore, finger-like voids and sponge like structures are not obtained in these samples. These results are consistent with the literature studies which showed that smaller particles yield finger-like structures [72, 116] and because of this reason, 316L particle size around 3-10 microns is preferred [71, 72, 76].

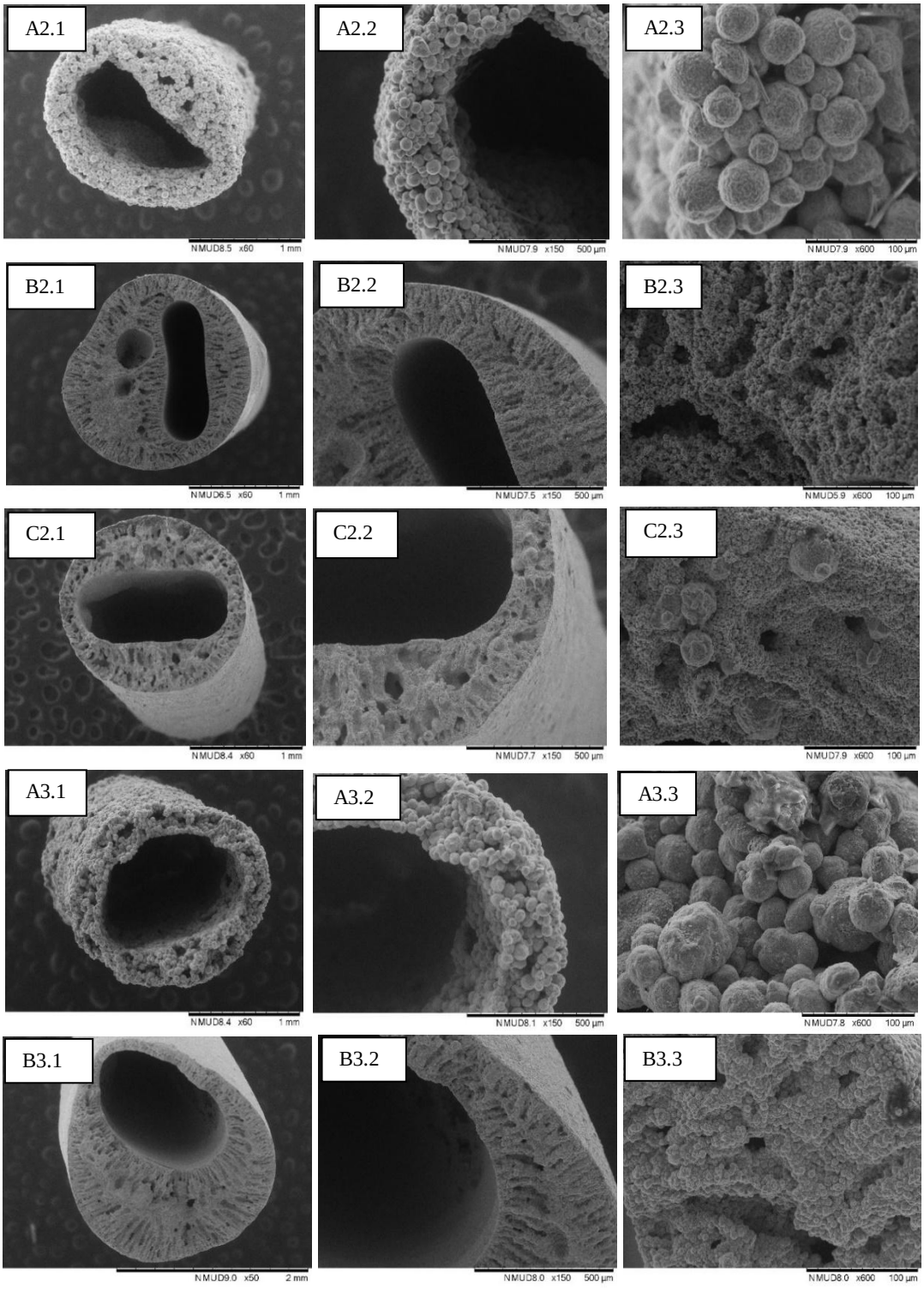

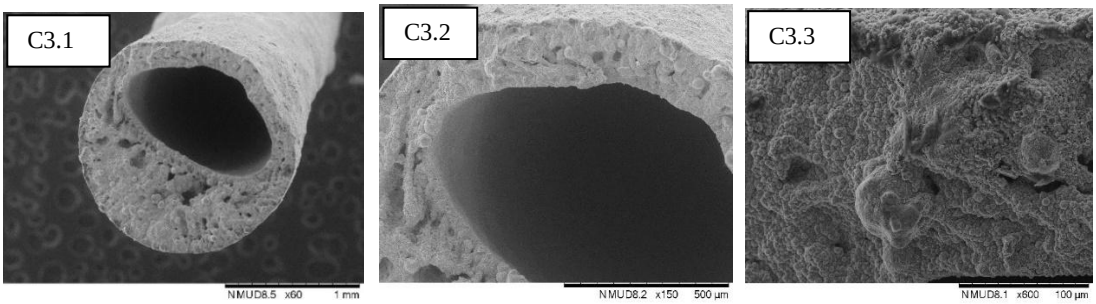

Figure 3.3 SEM Images Belong to N_2/H_2 Sintered Samples A2.1-2.3) C-SS, B2.1-2.3) F-SS, C2.1-2.3) M-SS, and Ar Sintered Samples A3.1-3.3) C-SS, B3.1-3.3) F-SS, C3.1-3.3) M-SS

Table 3.1 EDX analysis of N_2/H_2 sintered 316L SS hollow fiber membranes (in wt%).

Sample code	Fe	Cr	Ni	Mo	O	Si	N	C
C-SS	30	56	2	1	9	-	2	-
F-SS	56	34	6	1	1	-	1	-
M-SS	54	37	5	1	3	-	5	-

Figure 3.3 also gives the SEM images of argon atmosphere sintered 316L samples in order to evaluate the morphology of the fibers. Both spinning and sintering processes were performed successfully as the morphological properties were similar to the green HFs. HF samples have homogeneous hollow structure and shape. As a result of sintering process polymeric binder pyrolysed from HF structure like nitrogen atmosphere sintered samples.

Sponge like structures and finger like voids become dominant for the fine particle size HFs (F-SS). The finger-like structures are observed in B3.1 while sponge-like structures are observed for C3.1. For the samples with coarse particles A3.1-A3.3, large pores are obtained which is due to argon atmosphere and is parallel with the earlier findings [73]. Therefore, finger-like voids and sponge like structures are not obtained in these samples. These results are consistent with the literature studies which showed that smaller particles yield finger-like structures [72, 116] and because of this reason, 316L particle size around 3-10 microns is preferred [71, 72, 76].

Table 3.2 shows the EDX analysis of the Ar sintered 316L HF membranes having different particle size. Both compositions contain the major components of SS such as Fe, Cr, Ni, Mo.

Table 3.2 EDX Analysis of Ar Sintered 316L SS Hollow Fiber Membranes (in wt%).

Sample Code	Fe	Cr	Ni	Mo	O	Si	N	C
C-SS	36	54	2	1	7	-	-	-
F-SS	79	9	1	1	10	-	-	-
M-SS	60	24	8	2	6	-	-	-

Table 3.3 shows the diameters of 316L hollow fiber membranes. As a result, diameters of fibers are decreased with sintering due to shrinkage of the material. N_2/H_2 sintered F-SS sample has lower diameters than Ar sintered F-SS sample.

Table 3.3 Diameters of Hollow Fiber Membranes.

NON SINTERED	ID (mm)	OD (mm)	N_2/H_2 SINTERED	ID (mm)	OD (mm)	Ar SINTERED	ID (mm)	OD (mm)
C-SS	1.62	2.31	**C-SS**	1.55	1.87	**C-SS**	1.45	1.86
F-SS	1.73	2.29	**F-SS**	1.45	1.68	**F-SS**	1.70	2.10
M-SS	1.80	2.16	**M-SS**	1.50	1.71	**M-SS**	1.39	1.70

Table 3.4 shows the densification of 316L hollow fiber membranes. As a result, N_2/H_2 sintered 316 L samples give high densification than Ar sintered 316L samples.

Table 3.4 Densification of Sintered Hollow Fiber Membranes.

N_2/H_2 SINTERED	Shrinkage	Ar SINTERED	Shrinkage
C-SS	40%	**C-SS**	49%
F-SS	32%	**F-SS**	55%
M-SS	47%	**M-SS**	67%

3.2.2 X-Ray Diffraction Analysis

XRD analysis was performed to 316L HF samples sintered at 1150ºC at N_2/H_2 and argon atmospheres are shown in Figure 3.4. According to the analysis, all peaks belong to austenite phase, Cr_2O_3, Cr_7C_3 and $FeCr_2O_4$ phase of N_2/H_2 sintered HF membranes. As a result of sintering, the phases formed after the sintering process seem similar among all particle size compositions. Also, intensities of all phases are similar. Therefore, one analysis is given corresponding to all compositions.

According to the analysis of Ar sintered 316L samples, all peaks belong to austenite phase, Cr_2O_3, Cr_7C_3 and $FeCr_2O_4$ phase of Ar sintered HF membranes. The ratio of Cr_7C_3 and $FeCr_2O_4$ are slightly higher than the N_2/H_2 atmosphere. Since this chromium carbide is formed, it seems that some binders remain in the fiber sintered in argon atmosphere. Also, since the oxide phase is a bit too much, it appears to be a weak in preventing oxidation. At this point, it appears that hydrogen in the nitrogen atmosphere has a positive contribution to reducing oxides. Also, phase contents appear to be quite similar.

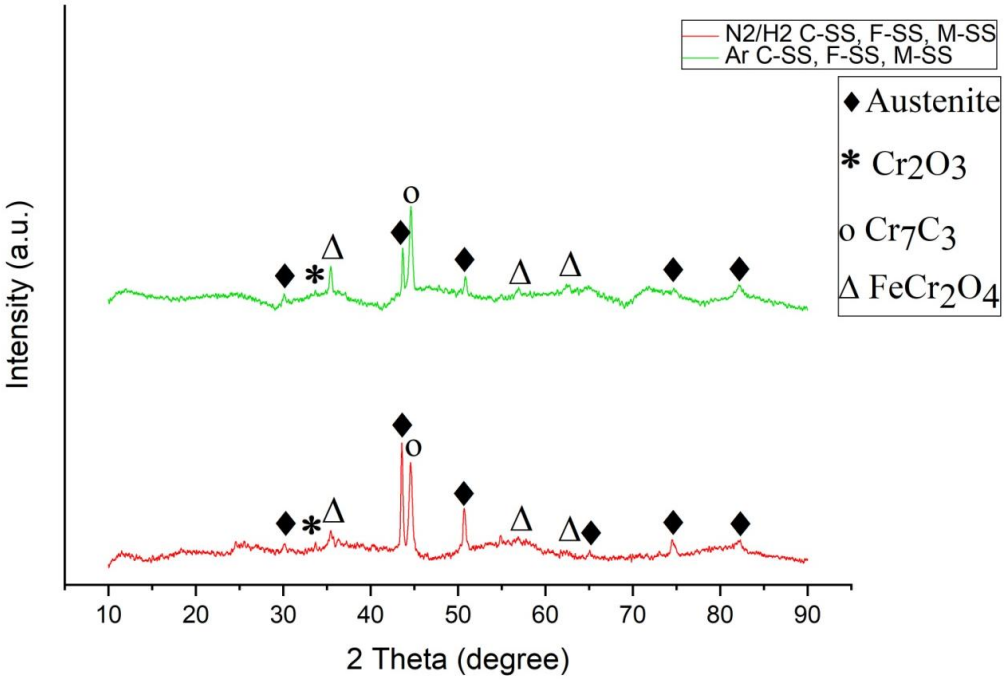

Figure 3.4 XRD Results of N_2/H_2 and Ar Sintered 316L Samples

3.2.3 Electrical Resistivity Measurements

Table 3.5 shows the electrical resistance of the 316L hollow fibers as function of the particle size and sintering atmosphere. The electrical resistance decreases with decreasing starting particle size as finest and mixed particle sizes give lower values for both atmospheres compared to coarse particle size.

When the sintering atmospheres are compared, argon atmosphere gives higher electrical resistivity than nitrogen atmosphere. Also, mixed particles size gives lower resistivity value for N_2/H_2 atmosphere whereas finest particle size gives the lowest value for argon atmosphere. The lower pore size creates a conductive path and as a result denser structure (lower resistance) is obtained. High standart deviation values can be because of the porous nature of the HF samples. N_2/H_2 sintered M-SS has lowest electrical resistivity. Fine particles samples (F-SS) of Ar atmosphere has lowest electrical resistivity.

Table 3.5 Electrical Resistivity Analysis of N_2/H_2 and Ar Sintered SS Hollow Fiber Membranes.

SAMPLE (10 mm)	N_2/H_2 atm electrical resisvity	Ar atm electrical resisvity
C-SS	1.40 Ω ± 0.36	2.85 Ω ± .35
F-SS	1.43 Ω ± 0.15	1.45 Ω ± .49
M-SS	1.03 Ω ± 0.30	1.70 Ω ± .84

3.2.4 Mercury Porosimeter Analysis

Table 3.6 shows the percentage porosity and average pore diameter values of N_2/H_2 sintered samples. As the particles sizes are decreased in C-SS, F-SS and M-SS samples, the amount of porosity decreases from 58 to 50 and 37 % respectively which means samples with finer particles give denser structures with lower porosity.

Table 3.6 Pore Analysis of Ar and N_2/H_2 Sintered 316L Hollow Fiber Membranes.

Sample Code	Porosity% - N_2/H_2 sintered	Porosity% - Ar sintered	Average Pore Diameter (µm) – N_2/H_2 sintered	Average Pore Diameter (µm) – Ar sintered
C-SS	58.04	55.34	29.50	4.60
F-SS	50.94	44.74	1.20	1.40
M-SS	37.94	41.21	1.30	1.20

The pore size distribution of N_2/H_2 sintered sample is shown in Figure 3.5. C-SS has coarse particles so there are also large pores in the structure. F- SS and M-SS have pore diameter distribution between 1-10 micron size. Also, M-SS contains high amount of pores with 1-5 micron size. As a result, F-SS has more homogeneous distribution.

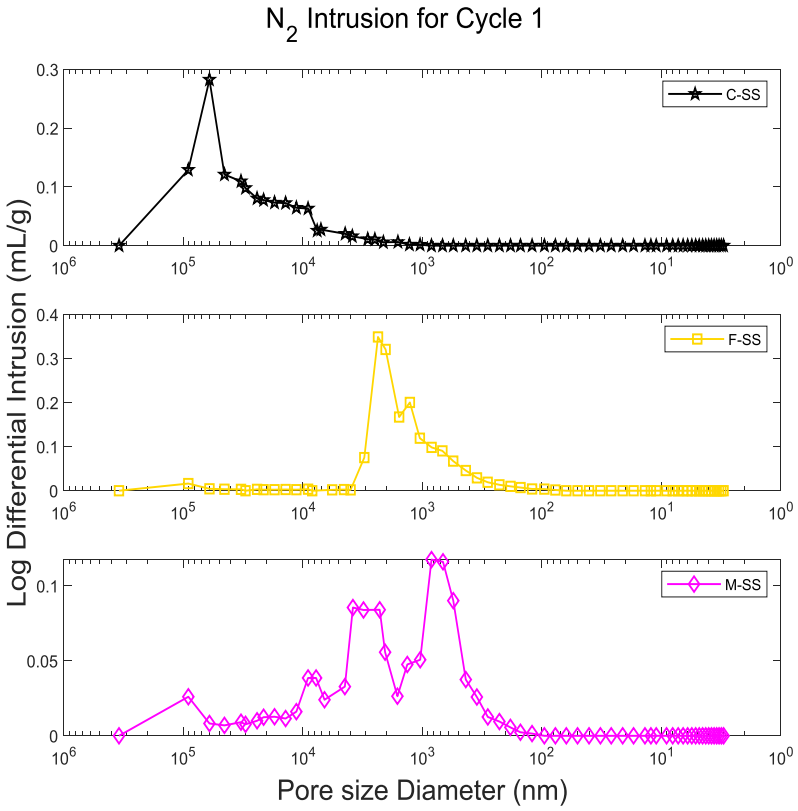

Figure 3.5 The Pore Size Distribution of N_2/H_2 Sintered 316L Samples

Also, mercury porosimetry analyzer was used to analyse of the pore size distribution of Ar sintered 316L samples, as given in Table 3.6. As the particles sizes are decreased, the amount of porosity decreases which means samples with finer particles give denser structures with lower porosity. This situation is also seen for the average pore diameter as they are decreased from 4.60 to 1.20 microns. In the study of Allioux et al. [76], it was shown that the pore size is smaller when multimodal size particles are used. So, the smaller pore size obtained for mixed particle size is similar as it is lower than the finest particle size. This can be interpreted as the sintering under N_2/H_2 atmosphere results in denser structures compared to Ar sintering.

The pore size distribution of Ar sintered C-SS sample has wide range between 1-30 micron which is shown in Figure 3.6. Result of Ar sintered F- SS is similar to the N_2/H_2 sintered F-SS sample. M-SS has 1-10 micron pore diameter distribution containing high percentage of 1-5 microns. This shows that the effectiveness of the sintering mechanism is little lower in argon atmosphere.

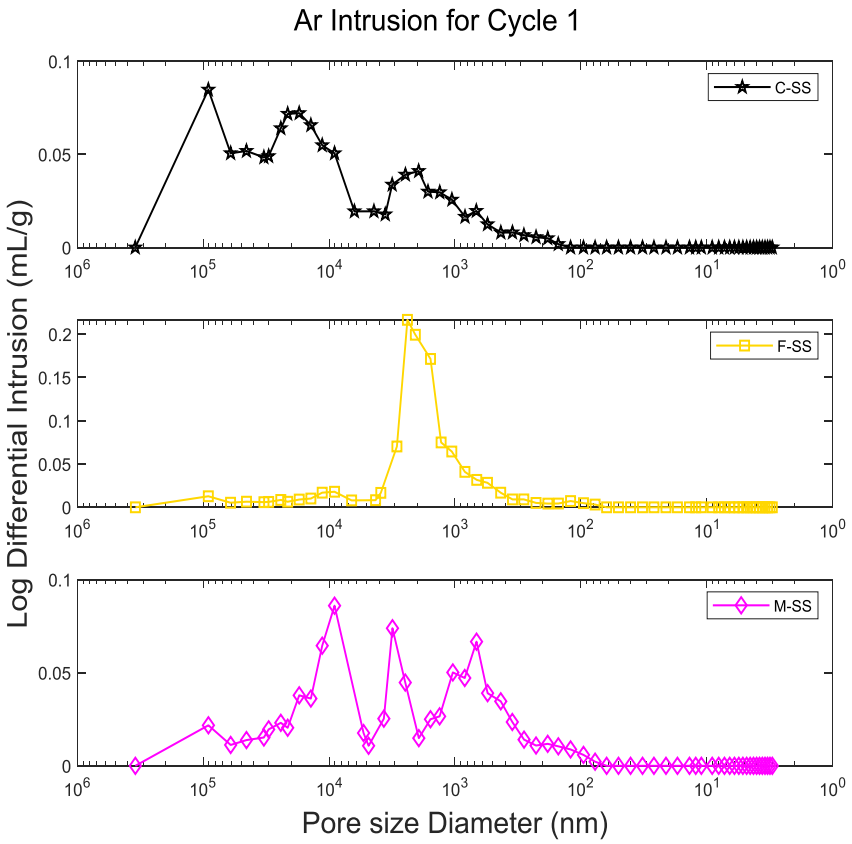

Figure 3.6 The Pore Size Distribution of Ar Sintered 316L Samples

3.2.5 Bending Test Analysis

Table 3.7 shows the bending test analysis of Ar and N_2/H_2 sintered 316L hollow fiber membranes. Coarse particles which are Ar sintered C-SS and N_2/H_2 sintered C-SS have lower bending strength and bending deflection. Also, N_2/H_2 sintered samples have lower bending strength and deflection than Ar sintered samples. The higher % porosity in N_2/H_2 sintered samples found as a result of mercury porosimetry analysis confirms this result. Fine particle sizes samples show higher bending strength and bending deflection compared to coarse and mixed particle size samples. Particle size has an impact on mechanical strength. In this study, results of 316L HFs shows parallel mechanical properties compared with the results of study of Ming Wang et al [118], and the other studies in the literature [63, 116]. The values are slightly lower than the literature. However, in this study, as in the literature, as the particle size decreases, the strength increases.

Table 3.7 Bending Test Analysis of Ar and N_2/H_2 Sintered 316L Hollow Fiber Membranes.

SAMPLE CODE	Bending Strength (MPa)	Bending Deflection (mm)
Ar sintered C-SS	26.7 ± 2.1	1.3 ± 0.1
Ar sintered F-SS	250.2 ± 25.1	6.1 ± 1.2
Ar sintered M-SS	212.5 ± 29.9	6.0 ± 0.6
N_2/H_2 sintered C-SS	22.2 ± 1.2	0.8 ± 0.1
N_2/H_2 sintered F-SS	208.6 ± 45.5	2.1 ± 0.15
N_2/H_2 sintered M-SS	200.4 ± 15.9	1.4 ± 0.06

3.2.6 Gas Permeability Analysis

Table 3.8 shows the results of gas permeability analysis of Ar and N_2/H_2 sintered 316L hollow fiber membranes. The permeability of Ar sintered samples increased from $9.34x10^{-6}$mol m^{-2} s^{-1} Pa^{-1} to $49.35x10^{-6}$mol m^{-2} s^{-1} Pa^{-1}. Ar sintered coarse particles have higher N_2 permenance due to larger pores. Mixed particles have lowest N_2 permenance because small particles fill the pores between large particles. The permeability of N_2/H_2 sintered samples increased from $19.97x10^{-6}$mol $m^{-2}s^{-1}Pa^{-1}$ to $97.87x10^{-6}$mol $m^{-2}s^{-1}Pa^{-1}$. N_2/H_2 sintered coarse particles have higher N_2 permenance due to larger pores. Mixed particles have lowest N_2 permenance because small particles fill the pores between large particles. Results are similar to the literature [63, 71, 72, 119].

Table 3.8 Gas Permeability Analysis of Ar and N_2/H_2 Sintered 316L Hollow Fiber Membranes.

SAMPLE CODE	Gas Permeability (10^{-6}mol m^{-2} s^{-1} Pa^{-1})
Ar Sintered C-SS	49.35
Ar Sintered F-SS	14.32
Ar Sintered M-SS	9.34
N_2/H_2 sintered C-SS	97.87
N_2/H_2 sintered F-SS	43.5
N_2/H_2 sintered M-SS	19.97

3.3 Sintered Composite Samples

Figure 3.7 shows the images of unsintered and sintered composite samples.

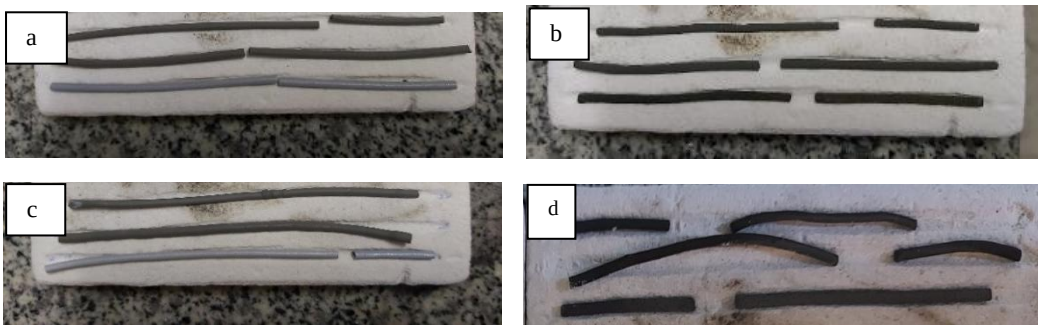

Figure 3.7 Composite Samples, a) Unsintered, b) Sintered in N_2/H_2 Atmosphere, c) Unsintered, d) Sintered in Ar Atmosphere

3.3.1 Scanning Electron Microscope and EDX Analysis

Figure 3.8 shows the SEM images from the cross-sections of N_2/H_2 and Ar sintered composite samples, respectively. It is clear that both spinning and sintering processes have been performed successfully since HF samples have homogeneous hollow structure and shape.

For the sintering applied in nitrogen-hydrogen atmosphere which has a potential of preventing from oxidation as well as some amount of chromium nitride formation, it seems all the polymeric binder pyrolysed from HF structure. When particle sizes are compared, membrane with finest particles has higher densification in terms of microstructure, also have a dominant finger-like structure but also some sponge-like structures. These two structures are typical signs of hollow fibers. The finger-like structure occurs from inner surface, the sponge-like structures are located at the outer region of the cross-section [73]. The finger-like voids were generated due to fast exchange between solvent (NMP) and no-solvent (water) while sponge-like structure was formed due to slow exchange during the spinning process [118]. For the mixed particle size HFs (M-COMP), sponge like structures and voids become dominant. Nevertheless, the finger-like structures are observed for only F-COMP while the macrovoids with sponge-like structures are observed for M-COMP. For the samples with coarse particles, large pores are obtained belong to C-COMP. Desired finger-like voids and sponge like structures are not obtained in these samples. These results are consistent with the literature studies which showed that smaller particles yield finger-like structures [72], and therefore researcher prefer to use a 316L particle size around 3-10 microns [71, 72, 76]. Also, these results show that, contrary to the existing literature, the structure of macro voids is affected more importantly by the particle size not by the solid loading content.

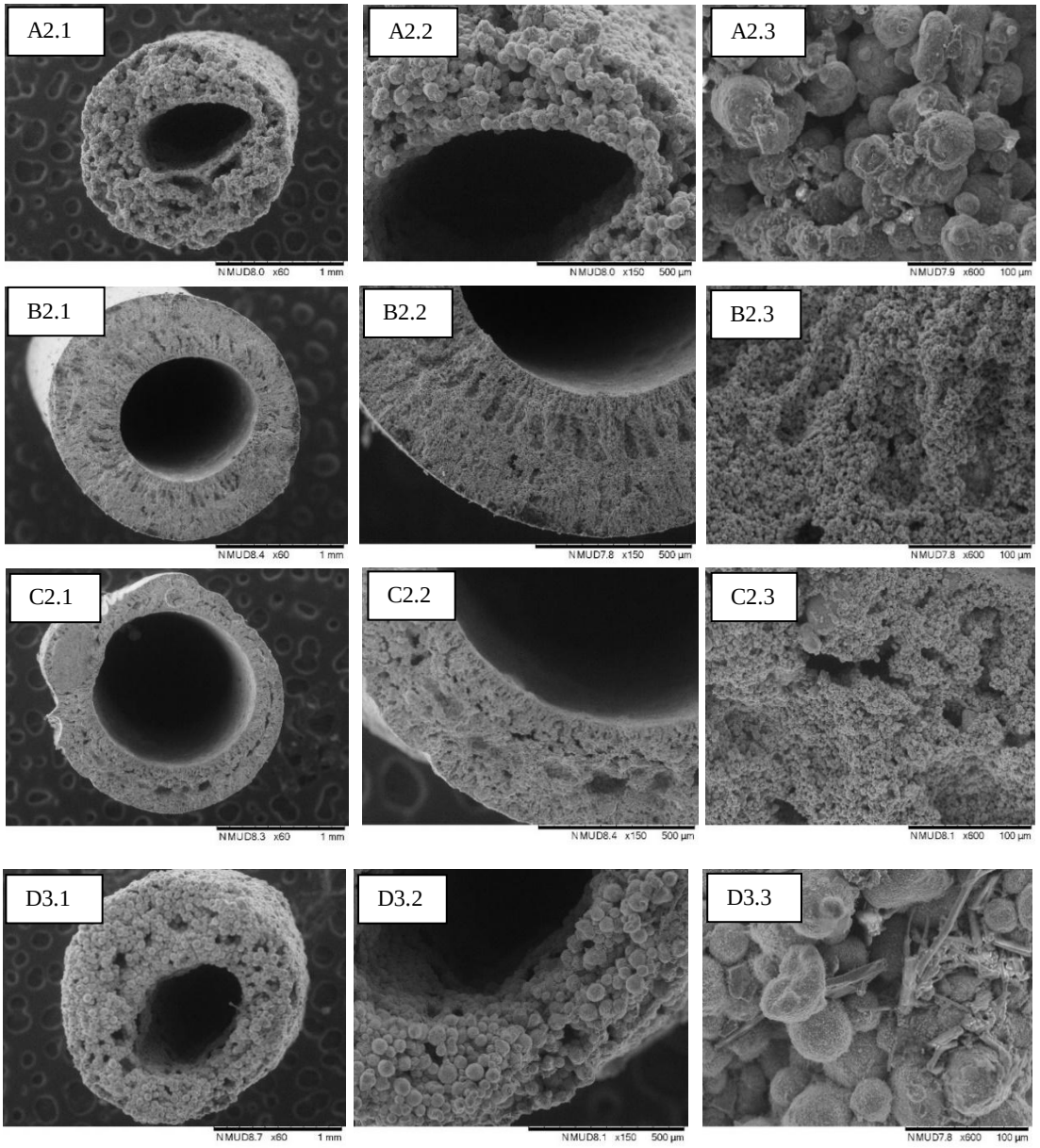
A2.1
A2.2
A2.3
B2.1
B2.2
B2.3
C2.1
C2.2
C2.3
D3.1
D3.2
D3.3

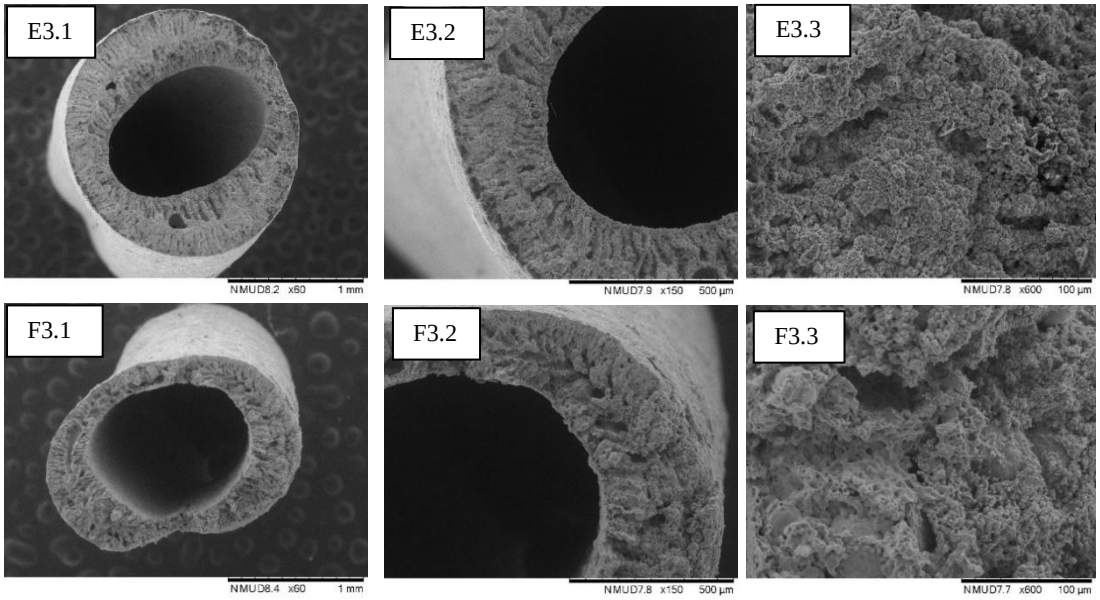

Figure 3.8 SEM Images Belong to N_2/H_2 Sintered Samples A2.1-2.3) C-COMP, B2.1-2.3) F-COMP, C2.1-2.3) M-COMP, and Ar Sintered Samples D3.1-3.3) C-COMP, E3.1-3.3) F-COMP, F3.1-3.3) M-COMP.

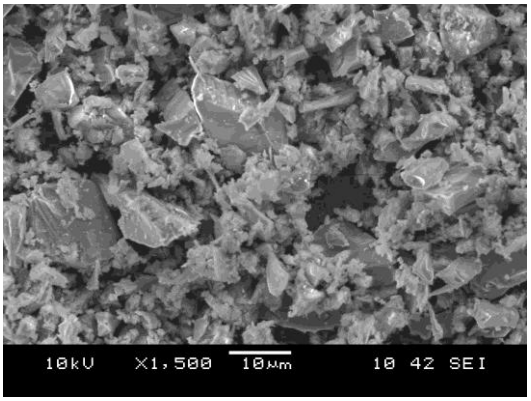

Figure 3.9 SEM Image of SiC Particles

Figure 3.9 shows the SEM image of SiC particles. Table 3.9 shows the EDX analysis of N_2/H_2 sintered HF samples having different particle size. All compositions contain the major components of SS such as Fe, Cr, Ni, and Mo. Also, analysis of composite HF membranes contains Si and C elements due to the presence of SiC [15]. One important point here is that a small amount of carbon is present in the structures, similar to the findings of Rui et al. [11], and this residual carbon might be a result of nitrogen sintering. Moreover, the oxygen content is near zero, which could be attributed to the presence of hydrogen in the sintering atmosphere composition.

Table 3.9 EDX Analysis of N_2/H_2 Sintered Hollow Fiber Membranes (Elemental Compositions in wt%).

Sample code	Fe	Cr	Ni	Mo	O	Si	N	C
C-COMP	41	27	4	1	-	27	-	1
F-COMP	45	34	5	1	-	11	-	3
M-COMP	43	37	4	2	-	7	1	3

Figure 3.8 also gives the SEM images of argon atmosphere sintered samples in order to evaluate the morphology of the fibers. Both spinning and sintering process was performed successfully as the morphological properties were similar to the green HFs. HF samples have homogeneous hollow structure and shape. As a result of sintering process polymeric binder pyrolysed from HF structure like nitrogen atmosphere sintered samples. Composite HF membrane with finest particle size has higher densification in terms of microstructure, also it is seen that F-COMP samples have the finger-like structure both in the inner and outer part of the fiber. And, mixed particle size results in both finger-like structures is together with the sponge-like structure. There are some large pores in the centre of the hollow fibers for M-COMP samples, which is due to argon atmosphere and is parallel with the earlier findings [73]. Finger-like and sponge like structures are not obtained from C-COMP samples, and large pores are obtained similar to nitrogen atmosphere sintering.

Table 3.10 shows the EDX analysis of the Ar sintered HF samples and the intermediate phase. Both compositions contain the major components of SS such as Fe, Cr, Ni, and Mo. Also, composite HF membranes contain Si and C due to the presence of SiC. The higher amount of carbon in the mixed particle sized sample shows that SiC decomposition took place as there is some amount of free carbon. And also some oxidation of carbon and silicon takes place similar to the earlier findings with 316L/SiC systems [15].

Table 3.10 EDX Analysis of Ar Sintered HF (Elemental Compositions in wt%).

Sample code	Fe	Cr	Ni	Mo	O	Si	N	C
C-COMP	37	41	2	-	-	21	-	-
F-COMP	56	20	7	1	6	10	-	-
M-COMP	50	2	1	-	13	2	-	32

Table 3.11 shows the diameters of composite hollow fiber membranes. As a result, diameters of fibers are decreased with sintering due to shrinkage of the material.

Table 3.11 Diameters of Composite Hollow Fiber Membrane Samples.

NON SINTERED	ID (mm)	OD (mm)	N_2/H_2 SINTERED	ID (mm)	OD (mm)	Ar SINTERED	ID (mm)	OD (mm)
C-COMP	1.45	2.32	**C-COMP**	1.05	1.61	**C-COMP**	1.16	1.70
F-COMP	1.62	2.33	**F-COMP**	1.13	1.50	**F-COMP**	1.46	1.76
M-COMP	1.50	2.30	**M-COMP**	1.41	1.72	**M-COMP**	1.38	1.62

Table 3.12 shows the densification of composite hollow fiber membranes. M-COMP give lower percentage of reduction due to different particle sizes. C-COMP sintered samples have large pore due to coarse particle sizes. Therefore C-COMP samples give higher percenrage of reduction.

Table 3.12 Densification of Sintered Composite Hollow Fiber Membranes.

N_2/H_2 SINTERED	Shrinkage	Ar SINTERED	Shrinkage
C-COMP	45%	C-COMP	47%
F-COMP	35%	F-COMP	34%
M-COMP	31%	M-COMP	32%

3.3.2 X-Ray Diffraction Analysis

XRD analysis was performed to 316L/SiC HF samples sintered at 1150ºC at N_2/H_2 and argon atmospheres are shown in Figure 3.10. According to the analysis, all peaks belong to austenite phase, Cr_2O_3, Cr_7C_3, $FeCr_2O_4$ and SiC phase of N_2/H_2 sintered HF membranes. As a result of sintering, N_2 sintered samples at different phase contents and their intensities appear to be quite similar, and no phase change.

According to the analysis of Ar sintered samples, all peaks belong to austenite phase, Cr_2O_3, Cr_7C_3, $FeCr_2O_4$ and SiC phase of Ar sintered HF membranes. Phase contents and their intensities appear to be quite similar, only there is more amount of chromium carbide in the nitrogen sintered samples which is consistent with the EDX analysis (as in Table 3.8).

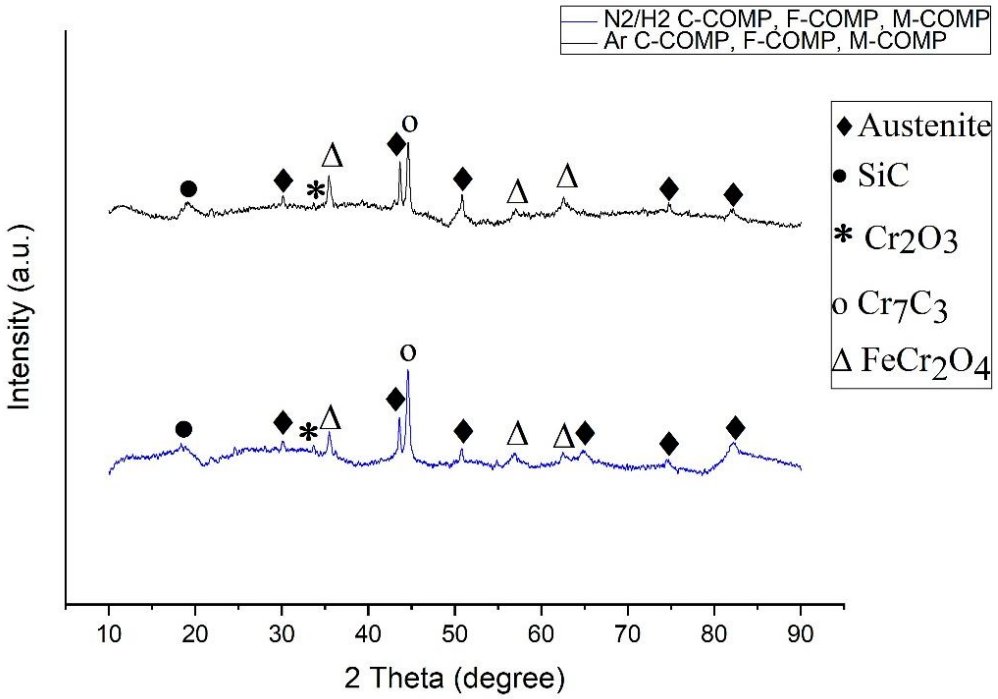

Figure 3.10 XRD Results of N_2/H_2 and Ar Sintered Samples

3.3.3 Electrical Resistivity Measurements

Table 3.13 shows the electrical resistance of the different compositions of 316L/SiC composite hollow fibers as function of the particle size and sintering atmosphere. The electrical resistance decreases with decreasing starting particle size as finest and mixed particle sizes give lower values for both atmospheres compared to coarse particle size. This is because the lower pore size creates a conductive path and as a result denser structure (lower resistance) is obtained.

When the sintering atmospheres are compared, argon atmosphere gives higher electrical resistivity than nitrogen atmosphere. Also, mixed particles size gives lower resistivity value for N_2/H_2 atmosphere whereas finest particle size gives the lowest value for argon atmosphere. The lower pore size creates a conductive path and as a results denser structure (lower resistance) is obtained. Therefore, fine particles samples of Ar atmosphere (F-COMP) have lowest electrical resistivity However, there is no big difference observed between F-COMP and M-COMP samples because the standard deviations are considerably high. These high standard deviation values can be because of the porous nature of the HF samples.

Table 3.13 Electrical Resistivity Analysis of N_2/H_2 and Ar Sintered 316L/SiC Composite Hollow Fiber Membranes.

Sample code (10 mm)	**Electrical resistivity N_2/H_2 atmosphere**	**Electrical resistivity Ar atmosphere**
C-COMP	1.53 Ω ± 0.20	2.30 Ω ± 0.28
F-COMP	1.30 Ω ± 0.20	1.85 Ω ± 0.77
M-COMP	1.16 Ω ± 0.35	2.20 Ω ± 0.55

3.3.4 Mercury Porosimeter Analysis

The percentage porosity and average pore diameter values of N_2/H_2 sintered samples are given in Table 3.14. As the particles sizes are decreased in F-COMP and M-COMP samples, the amount of porosity decreases significantly from 49 to 35 and 39 % which means samples with finer particles give denser structures with lower porosity. This situation is also seen for the average pore diameter as they are decreased from 14.9 to 0.98 and 0.66 microns. In the study of Allioux et al. [76], it was shown that the pore size is smaller when multimodal size particles are used. So, the smaller pore size obtained for mixed particle size is similar as it is lower than the finest particle size.

Table 3.14 Pore Analysis of the Sintered Hollow Fiber Membranes.

Sample code	Porosity% - N_2/H_2 sintered	Porosity% - Ar sintered	Average Pore Diameter (µm) – N_2/H_2 sintered	Average Pore Diameter (µm) – Ar sintered
C-COMP	49.37	56.94	14.9	11.8
F-COMP	35.49	40.04	0.98	2.3
M-COMP	39.19	33.29	0.66	2.3

The pore size distribution of N_2/H_2 sintered sample is shown in Figure 3.11. C-COMP has coarse particles so there are also large pores in the structure. F- COMP and M-COMP have pore diameter distribution between 1-10 micron size. However, even the M-COMP contains more amount of smaller submicron pores it has a heterogenous distribution containing also high amount of pores with 1-5 micron size. Different to that situation, F-COMP has more homogeneous distribution.

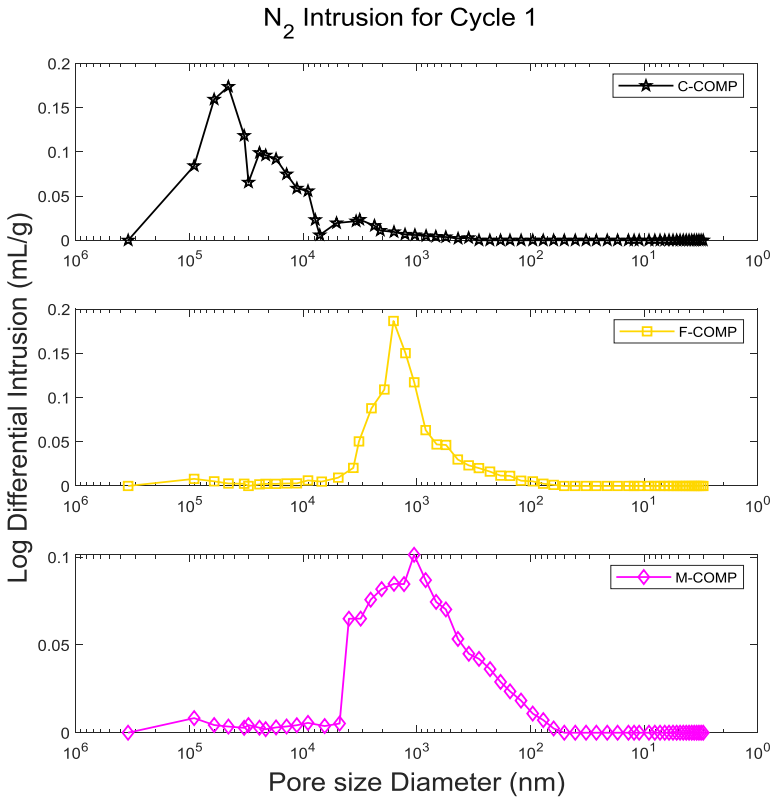

Figure 3.11 The Pore Size Distribution of N_2/H_2 Sintered Samples

Mercury porosimetry analyzer was used to analyses of the pore size distribution of Ar sintered samples, as given in Table 3.13. As the particles sizes are decreased in F-COMP and M-COMP samples, the amount of porosity decreases significantly from 57 to 40 and 33 % which means samples with finer particles gives denser structures with lower porosity. This situation is also seen for the average pore diameter as they are decreased from 11.8 to 2.3 microns. In the study of Allioux et al. [30], it was shown that the pore size is smaller when a multimodal size particles are used. These findings are similar with the findings obtained from N_2/H_2 atmosphere sintering except the average pore diameters values are considerably higher. This can be interpreted as the sintering under N_2/H_2 atmosphere results in denser structures compared to argon sintering.

The pore size distribution of C-COMP has wide range between 1-30 microns which is shown in Figure 3.12. Result of Ar sintered F- COMP is similar to the N_2/H_2 sintered F-COMP sample. M-COMP has 1-10 micron pore diameter distribution containing high percentage of 1-5 microns rather than submicron pores which is

different than the previous situation. This show that the effectiveness of the sintering mechanism is little lower in argon atmosphere.

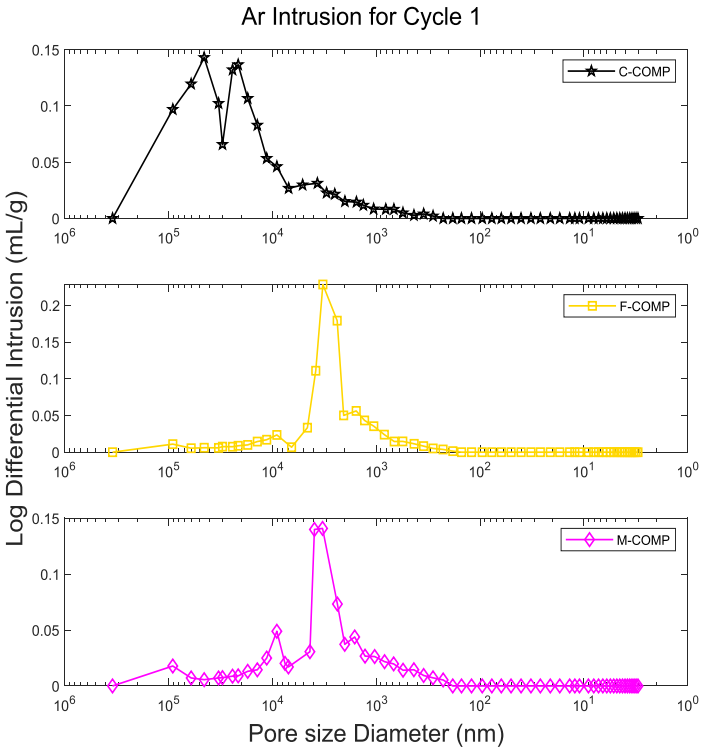

Figure 3.12 The Pore Size Distribution of Ar Sintered Samples

3.3.5 Bending Test Analysis

Table 3.15 shows the bending test analysis of Ar and N_2/H_2 sintered composite hollow fiber membranes. Coarse particles which are Ar sintered C-COMP and N_2/H_2 sintered C-COMP have the lowest bending strength and bending deflection compared to other particle sizes. And, the finest particle size samples have the highest bending strength and bending deflection. When the sintering atmospheres are compared, N_2/H_2 atmosphere gives comparable strength values yet the ductility is lower than Ar sintered samples. These results are parallel to the literature as the particle size has an importance on mechanical strength [118].

Table 3.15 Pore Analysis of Ar and N_2/H_2 Sintered Composite Hollow Fiber Membranes.

SAMPLE CODE	Bending Strength (MPa)	Bending Deflection (mm)
Ar sintered C-COMP	26.2 ± 0.7	1.2 ± 0.1
Ar sintered F-COMP	226.6 ± 28	3.7 ± 0.9
Ar sintered M-COMP	202.4 ± 24.4	2,7 ± 1.2
N_2/H_2 sintered C-COMP	23.5 ± 25.1	0.5 ± 0.15
N_2/H_2 sintered F-COMP	286.0 ± 17.6	2.0 ± 1.3
N_2/H_2 sintered M-COMP	200.1 ± 13.6	1.3 ± 0.4

3.3.6 Gas Permeability Analysis

Table 3.16 shows the results of gas permeability analysis of Ar and N_2/H_2 sintered composite hollow fiber membranes. The permeability of Ar sintered samples increased from $17.12x10^{-6}$mol m^{-2} s^{-1} Pa^{-1} to $195.75x10^{-6}$mol m^{-2} s^{-1} Pa^{-1}. Ar sintered coarse particles have higher N_2 permenance due to larger pores. Mixed particles have lowest N_2 permenance because small particles and SiC particles fill the pores between large particles. The permeability of N_2/H_2 sintered samples increased from $26.57x10^{-6}$mol $m^{-2}s^{-1}Pa^{-1}$ to $244.69x10^{-6}$mol $m^{-2}s^{-1}Pa^{-1}$. N_2/H_2 sintered coarse particles have higher N_2 permenance due to larger pores. Mixed particles have lowest N_2 permenance because small particles and SiC particles fill the pores between large particles. Results are similar to the literature [63, 71, 72, 119].

Table 3.16 Gas Permeability Analysis of Ar and N_2/H_2 Sintered Composite Hollow Fiber Membranes.

SAMPLE CODE	Gas Permeability (10^{-6}mol m^{-2} s^{-1} Pa^{-1})
Ar Sintered C-COMP	195.75
Ar Sintered F-COMP	40.78
Ar Sintered M-COMP	17.12
N_2/H_2 sintered C-COMP	244.69
N_2/H_2 sintered F-COMP	32.27
N_2/H_2 sintered M-COMP	26.57

4. CONCLUSIONS

Conclusions of sintered 316L samples are listed below;

316L samples were prepared for this study. Both spinning and sintering process was performed successfully. Polymeric binder pyrolysed from HF structure in both atmospheres. It has been observed that stainless steel HF samples had a homogeneous hollow structure and shape.

1) HF produced from fine particles have higher densification when particle sizes are compared. Also, they have dominant finger-like structure but also some sponge-like structures which are shown in SEM figures. For the samples with coarse particles, large pores are obtained, therefore, finger-like voids and sponge like structures are not obtained in coarse particles. These results are similar for both two atmosphere sintered samples. Therefore, 3-10 micron particle size should be preferred for production of hollow fiber membranes.
2) Nitrogen-hydrogen atmosphere has a potential of preventing from oxidation as well as some amount of chromium nitride formation. EDS results show the major components of N_2/H_2 sintered samples are Fe, Cr, Ni, Mo. and N. Also, EDS results show the major components of Ar sintered samples are Fe, Cr, Ni, Mo. It seems that all the polymeric binder pyrolysed from HF structure.
3) Therefore, N_2/H_2 sintered 316L F-SS sample has lower diameters than Ar sintered 316L F-SS sample.
4) N_2/H_2 sintered 316 L samples give high densification than Ar sintered 316L samples.

5) As a result of XRD analysis, all peaks belong to austenite phase, Cr_2O_3, Cr_7C_3 and $FeCr_2O_4$ phase of HF membranes for both N_2/H_2 and Ar sintered 316L samples. Phase contents and their intensities appear to be quite similar between two different sintering atmospheres.

6) As a result of electrical resistivity measurements, for both atmospheres, the electrical resistance decreases with decreasing particle size as finest (denser structure) and mixed particle sizes give lower values for both atmospheres compared to coarse particle size because lower pore size creates a conductive path. When the sintering atmospheres are compared, argon atmosphere gives higher electrical resistivity than nitrogen atmosphere.

7) As a result of mercury porosimeter analysis, for both atmospheres, when the particles sizes are decreased, the amount of porosity decreases which means samples with finer particles give denser structures with lower porosity. Coarse particles have large pores in the structure and mixed particle size 316L samples have smaller pore size. N_2/H_2 sintered 316L samples have denser structures than Ar sintered 316L samples. Also, the pore diameter distributions which are 1-10 microns are similar for both Ar sintered F- SS sample and N_2/H_2 sintered F-SS and M-SS samples.

8) As a result of bending test, coarse particles (C-SS) samples have the lowest bending strength and bending deflection for both two atmospheres. Also, fine particle sizes samples have higher bending strength and bending deflection. Also, Ar atmosphere results in higher bending strength and ductility compared to N_2/H_2 atmosphere.

9) Sintered 316L coarse particles (C-SS) have higher N_2 permenance due to large pores. Mixed particles have the lowest N_2 permenance because small particles fill the pores between large particles. Results of Ar and N_2/H_2 atmospheres are similar as particle size comparison. Argon atmosphere have lower gas permeability than hydrogen/nitrogen gas permeability.

Conclusions of sintered composite samples are listed below;

Also, composite samples were prepared for this study. Both spinning and sintering process was performed successfully. Polymeric binder pyrolysed from HF structure in both atmospheres. It has been observed that stainless steel composite HF samples have homogeneous hollow structure and shape.

1) As a result of SEM, for the mixed particle size (M-COMP) samples have sponge like structures and fingerlike voids. F-COMP samples have finger-like structures both in the inner and outer part of the fiber. For the samples with coarse particles (C-COMP) finger-like voids and sponge like structures are not obtained. These are result of both two atmospheres.
2) Composite HF membrane with finest particle size has higher densification.
3) As a result of EDS, all compositions contain the major components of SS such as Fe, Cr, Ni, Mo and analysis of composite HF membranes contains Si and C elements due to the presence of SiC for both two sintering atmospheres. For N_2/H_2 sintered samples, the oxygen content is near zero, which could be attributed to the presence of hydrogen in the sintering atmosphere composition.
4) M-COMP give lower percentage of reduction due to different particle sizes. C-COMP sintered samples have large pore due to coarse particle sizes. Therefore C-COMP samples give higher percentage of reduction.
5) As a result of XRD analysis, all peaks belong to austenite phase, Cr_2O_3, Cr_7C_3, $FeCr_2O_4$ and SiC phase of N_2/H_2 and Ar sintered samples. Only difference between two atmospheres is more amount of chromium carbide in N_2/H_2 sintered samples.
6) As a result of electrical resistivity analysis, the electrical resistance decreases with decreasing starting particle size. Fine and mixed particle sizes give lower values for both atmospheres compared to coarse particle size. Argon atmosphere gives higher electrical resistivity than N_2/H_2 atmosphere. Also, mixed particles size gives lower resistivity value for N_2/H_2 atmosphere whereas finest particle size gives the lowest value for argon atmosphere but there is no big difference observed between F-COMP and M-COMP samples because the standard

deviations are considerably high. These high standard deviation values can be because of the porous nature of the HF samples.

7) As a result of mercury porosimeter of both two atmospheres, samples with finer particles give denser structures with lower porosity. This situation is also seen for the average pore diameter, it decreases. smaller pore size obtained for mixed particle size is similar as it is lower than the finest particle size. F- COMP and M-COMP have pore diameter distribution between 1-10 micron size. The average pore diameters of Ar sintered samples are higher. This can be interpreted as the sintering under N_2/H_2 atmosphere results in denser structures compared to argon sintering.

8) As a result of bending test of both two atmospheres, coarse particles have lower bending strength and bending deflection. And also, Ar sintered samples have higher ductility than N_2/H_2 sintered samples.

9) Sintered composite coarse particles (C-COMP) have higher N_2 permenance due to large pores. Mixed particles have the lowest N_2 permenance because small particles and SiC particles fill the pores between large particles. Argon atmosphere have lower gas permeability than hydrogen/nitrogen gas permeability.

REFERENCES

1. Aslan M. Membran Teknolojileri. T.C. Çevre Ve Şehircilik Bakanlığı. 2016; 978-605-9351-02-7.

2. Strathmann H. Membrane Separation Processes: Ullmann's Encyclopedia of Industrial Chemistry; 2011.

3. Shen Zhen Dreamemway Environmental Products Co., Ltd.. Available from: dreamemmbrufro.en.made-in-china.com [2019].

4. Fard AK, Mckay G, Buekenhoudt A, Sulaiti HA, Motmans F, Khraisheh M, Atieh M. Inorganic Membranes Preparation and Application for Water Treatment and Desalination. Material (Basel). 2018;11(1):74.

5. Mergen G. Gas Permeation Properties of Poly(Arylene Ether Ketone) and Its Mixed Matrix Membranes with Polypyrrole: The Middle East Technical University; 2003.

6. AQUADYN® UA 1060 UF. Hollow Fiber Module for Water Filtration. Available from: https://youtu.be/k24ek7idvrg [2016].

7. Baker RW. Membrane Technology and Applications: Third Edition. John Wiley & Sons; 2012.

8. Abdullah N, Rahman MA, Othman MHD, Jaafar J, Ismail AF. Current Trends and Future Developments on (Bio-) Membranes. Elsevier; 2018.

9. Advantages of Asymmetric Membranes. Available From: Https://Www.Sterlitech.Com [2018].

10. Pal P. Introduction to the Arsenic Contamination Problem; Groundwater Arsenic Remediation. Treatment Technology and Scale UP. 2015;1-23.

11. Definition of a Membrane. Available from: https://synderfiltration.com/ learning-center/articles/introduction-to-membranes [2018].

12. Yürekli Y, Polatoğlu İ, Baştürk SB. Filtrasyon Membranların Üretim ve Karakterizasyon Yöntemleri. Celal Bayar Üniversitesi Fen Bilimleri Dergisi. 2015;11(2):175-181.

13. Wenten IG. Recent Development in Membrane and Its Industrial Applications. Membrane Technology in Oil and Gas Industry. Conference Paper. 2015.

14. Schematic Diagrams of Module Types for Most Membrane Applications. Available from: https://www.researchgate.net/figure/schematic-diagrams-of-module-types-for-most-membrane-applications_fig6_322848705 [2020].

15. Türker T. Gümüş Nanopartiküller ile Kompozit Ince Boşluklu Fiber (Hollow Fiber) Membran Üretimi, Karakterizasyonu ve Uygulaması: İstanbul Teknik Üniversitesi; 2013.

16. Ockwig NW, Nenoff TM. Membranes for Hydrogen Separation. Chemical Review. 2007;107(10):4078-4110.

17. Terpstra R.A., Van Eijk J.P.G.M., Feenstra F.K.. Method for the Production of Ceramic Hollow Fibers. 1998. US Patent No. 5,707,584.

18. Feng C., Khulbe, K.C., Matsuura, T., Ismail, A.F. Recent Progresses İn Polymeric Hollow Fiber Membrane Preparation, Characterization and Applications. Separation Purification Technology. 2013;111: 43–71.

19. Peng N., Widjojo N., Sukitpaneenit P., Teoh M.M., Lipscomb G.G., Chung T.S., Lai J.Y. Evolution Of Polymeric Hollow Fibers as Sustainable Technologies: Past, Present, and Future. Progress Polymer Science. 2012;37:1401–1424.

20. Kas R., Hummadi K. K., Kortlever R., De Wit P., Milbrat A., Luiten-Olieman M. W. J., Benes N. E., Koper M. T. M., Mul G.. Three-Dimensional Porous Hollow Fibre Copper Electrodes for Efficient and High-Rate Electrochemical Carbon Dioxide Reduction. Natural Communications. 2016;7:10748.

21. Basu S., Khan A. L., Cano-Odena A., Liu C. Q., Vankelecom I. F. J.. Membrane-Based Technologies for Biogas Separations. Chemical Society Reviews. 2010; 39:750-68.

22. Mahon, H, McLain E. A.. Permselective Hollow Fibers and Method of Making. 1968. Ca Patent 786,719.

23. Mclain, E.A., Mahon H.. Permselective Hollow Fibers and Method of Making. 1969. Us Patent 3,423,491.

24. Geary E. Jr.. Method of Manufacture of Fluid Separation Apparatus. 1969. Us Patent 344,2002.

25. Geary E. Jr.. Centrifugal Casting Apparatus for Forming a Cast Wall Member Extending Transversely Across an Elongated Bundle of Substantially Parallel Hollow Filaments of A Fluid Permeation Separation Apparatus. 1969. Us Patent 349,2698.

26. Henis M.S.. Multicomponent Membranes for Gas Separation. 1980. US Patent 423,0463.

27. Khulbe K.C., Fent C., Matsuura T., Khayet M.. Polymeric Hollow Fibers: State of the Art Review of Their Preparation, Characterization and Applications in Different Research Areas. Journal Applied Membrane Science & Technology. 2006;4:53-88.

28. Cabasso I., Klein E., Smith K.. Polysulfone Hollow Fibers Spinning and Properties. Journal Applied Polymer Science. 1976;20(9):2377-239 4.

29. Baker R.W.. Membrane Technology and Applications. John Wiley & Sons Ltd. 2004;191–354.

30. Mulder, J.. Basic Principles of Membrane Technology. Kluwer Academic. 1996;51–58.

31. Ran, F., Drioli E., Giorno L.. Encyclopedia of Membranes. Springer. 2016;1598–1600.

32. Ida S., Kobayashi S., Müllen K.. Encyclopedia of Polymeric Nanomaterials. Springer. 2014;1528–1534.

33. Liu X.M., Wang Z.H., Yu B., Cong H.L., Gao X.L., Guo X.Y.. PMMA Modified PVDF Hollow Fiber Ultrafiltration Membranes. Advanced Materials. 2012;465:229-233.

34. Hubadillah S.K., Othman M.H., Ismail A.F., Rahman M.A., Jaafar J., Iwamoto Y., Honda S., Dzahir M.I., Mohd Yusop M.Z.. Fabrication of Low Cost, Green Silica Based Ceramic Hollow Fibre Membrane Prepared from Waste Rice Husk for Water Filtration Application. Ceramics International. 2018;44(9):10498-10509.

35. Matsuura T., Feng K.K.C.. Recent Progresses in Polymeric Hollow Fiber Membrane Preparation, Characterization and Applications. Separation and Purification Technology. 2013;111.

36. Zhang Y., Zhao J., Chu H., Zhou X., Wei Y.. Effect of Modified Attapulgite Addition on the Performance of a PVDF Ultrafiltration Membrane. Desalination. 2014;344:71–78.

37. Huang Y., Huang Q.-L., Liu H., Zhang C.-X., You Y.-W., Li N.-N., Xiao C.-F.. Preparation, Characterization, and Applications of Electrospun Ultrafine Fibrous PTFE Porous Membranes. Journal Membrane Science. 2017;523:317–326.

38. Koros W.J., Paul D.R., Yampol'skii Y.P., Pinnau I.. Membrane Formation for Gas Separation Processes. CRC Press. USA 1994.

39. Sridhar S., Smitha B., Aminabhavi T.M.. Separation of Carbondioxide from Natural Gas Mixtures Through Polymer Membranes. Separation Purification Review. 2007;36:113-74.

40. Qin J.J., Chung T.S.. Effects of Orientation Relaxation and Bore Fluid Chemistry on Morphology and Performance of Polyethersulfone Hollow Fibers For Gas Separation. Journal Membrane Science 2004;229:1-9.

41. Chen H.Z., Xiao Y.C., Chung T.S.. Multi-Layer Composite Hollow Fiber Membranes Derived from Poly (Ethyleneglycol) (PEG) Containing Hybrid Materials for CO2/N2 Separation. Journal Membrane Science. 2011;38:211-220.

42. Harun Z., Hasan H.S.K., S., Yunos M.Z.. Effect of Thermodynamic Properties on Porosity of Ceramic Membrane Prepared by Phase Inversion. Applied Mechanics and Materials. 2014;575:31–35.

43. Hubadillah S.K., Othman M.H.D., Harun Z., Ismail A.F., Iwamoto Y., Honda S., Rahman M.A., Jaafar J., Gani P., Mohd Sokri M.N.. Effect of Fabrication Parameters on Physical Properties of Metakaolin-Based Ceramic Hollow Fibre Membrane. Ceramics International. 2016;42:15547–15558.

44. Hubadillah S.K., Othman M.H.D., Harun Z., Ismail A.F., Salleh W.N.W., Basri H., Yunos M.Z., Gani P.. Preparation and Characterization of Low Cost Porous Ceramic Membrane Support from Kaolin Using Phase Inversion/Sintering Technique for Gas Separation: Effect of Kaolin Content and Non-Solvent Coagulant Bath. Chemical Engineering Research and Design. 2016;112:24–35.

45. Qiu W.L., Zhou F.B., Kosuri M.. Dehydration of Ethanol-Water Mixtures Using Asymmetric Hollow Fiber Membranes from Commercial Polyimides. Journal Membrane Science. 2009;327:96–103.

46. Arunima S., Bijay P., Mahendra K., Vinod K.. Membrane-Based Techniques for the Separation and Purification of Proteins: An Overview. Advances in Colloid and Interface Science. 2009;145:1–22.

47. Lu S., Chung T.S., Alan R.. Polymeric Membranes for the Hydrogen Economy: Contemporary Approaches and Prospects for the Future. Journal Membrane Science. 2009;327:18–31.

48. Wang T., Zhang Y., Li G., Li H.. Preparation and Characterization of Alumina Hollow Fiber Membranes. Frontiers in Chemical Engineering. 2009;3(3):265–271.

49. Lai C.Y., Groth A., Gray S., Duke M.. Enhanced Abrasion Resistant PVDF/Nanoclay Hollow Fibre Composite Membranes for Water Treatment. Journal Membrane Science. 2014;449:146–157.

50. Abdullah N., Rahman M.A., Othman M.H., Ismail A.F., Jaafar J., Aziz A.. Preparation and Characterization of Self-Cleaning Alumina Hollow Fiber Membrane Using The Phase Inversion and Sintering Technique. Ceramics International. 2016;42(10):12312-12322.

51. Lee M., Wu Z., Wang R., Li K.. Microstructured Alumina Hollow Fibre Membranes Potential Applications in Waste Water Treatment. Journal Membrane Science. 2014;461:39–48.

52. Paiman S.H., Rahman M.A., Othman M.H.D., Ismail A.F., Jaafar J., Azian A.A.. Morphological Study of Yttria-Stabilized Zirconia Hollow Fibre Membrane Prepared Using Phase Inversion/Sintering Technique. Ceramics International. 2015;41:12543–12553.

53. Zhang X., Hu J., Chang Q., Wang Y., Zhou J., Zhao T.. Influences of Internal Coagulant Composition on Microstructure and Properties of Porous YSZ Hollow Fibre Membranes for Water Treatment. Separation Purification Technology. 2015;147:337–345.

54. Oliveira S.S.L., Oliveira S.L, Ferreira R.S.B, Lirab H.L., Santana L.N.L., Araúj E.M.. Development of Hollow Fiber Membranes with Alumina and Waste of Quartzite. Materials Research. 2019:22;1.

55. Menezes R.R., Fagury-Neto E., Fernandes M.C., Souto P.M., Kiminami R.H.G.A.. Obtaining Porous Mullite from Rice Husk Silica and Aluminum Acetate. Ceramics. 2008;54(330):245-252.

56. Li L., Chen M., Dong Y., Dong X., Cerneaux S., Hampshire S.. A Low-Cost Alumina-Mullite Composite Hollow Fiber Ceramic Membrane Fabricated via Phase-Inversion and Sintering Method. Journal of the European Ceramic Society. 2016;36(8):2057-2066.

57. Liu Q., Xue T., Yang L., Hu X., Du H.. Controllable Synthesis of Hierarchical Porous Mullite Fiber Network for Gas Filtration. Journal of the European Ceramic Society. 2016;36(7):1691-1697.

58. Bai C.Y., Li Y., Liu Z.M., Liu P.W., Deng X.Y., Li J.B.. Fabrication and Properties of Mullite-Bonded Porous Sic Membrane Supports Using Bauxite As Aluminum Source. Ceramics International. 2015;41(3 Pt B):4391-4400.

59. Su C., Xu Y., Zhang W., Liu Y., Li J.. Porous Ceramic Membrane with Superhydrophobic and Superoleophilic Surface for Reclaiming Oil from Oily Water. Applied Surface Science. 2012;258:2319–2323.

60. Okon E., Shehu H., Gobina E.. Evaluation of the Performance of Alumina Nanoporous Ceramic Composite Membrane for Esterification Applications in Petroleum Refinery. Catalysis Today. 2017;310:146-156.

61. Lü Q., Dong X., Zhu Z., Dong Y.. Environment-Oriented Low-Cost Porous Mullite Ceramic Membrane Supports Fabricated from Coal Gangue and Bauxite. The Journal of Hazardous Materials. 2014;273:136–145.

62. Zhu L., Chen M., Dong Y., Tang C.Y., Huang A., Li L.. A Low-Cost Mullite-Titania Composite Ceramic Hollow Fiber Microfiltration Membrane for Highly Efficient Separation of Oil-In-Water Emulsion. Water Research. 2016;90:277–285.

63. Rui W, Zhang C, Cai C, Gu X. Effects of Sintering Atmospheres on Properties of Stainless Steel Porous Hollow Fiber Membranes. Journal of Membrane Science. 2015;489:90-97.

64. Cassano A, Rastogi NK, Basile A. Advances in Membrane Technologies for Water Treatment. Woodhead Publishing, Oxford, UK. 2015;551–580.

65. Ertugrul O, Park HS, Porada MW. Effect of Particle Size and Heating Rate in Microwave Sintering of 316L Stainless Steel. Powder Technology. 2014; 253:703-709.

66. Arık H. Investigation of Wear Properties of Al-SiC Composite Materials Produced by Powder Metallurgy Method. Fen Bilimleri Dergisi. 2019;741-754.

67. Patankar SN, Chandrasekaran M, Tan MJ. Matrix Reinforcement Interaction in SiC/316L Stainless Steel Composite. Journal Materials Science Letters. 2000;19:613–615.

68. Mima S, Yodkaew T, Morakotjinda M, Tosangthum N, Daraphan N, Krataitong R, Coovattanachai O, Vetayanugul B, Tongsri R. The Fourth Thailand Materials Science and Technology Conferance, Available from: http://www2.mtec.or.th/th/seminar/ msativ/pdf/m07.pdf [2006].

69. Klar E, Samal PK. Powder Metallurgy Stainless Steels: Processing, Microstructures, and Properties. ASM International, Materials Park, OH. 2007;256.

70. Kato T, Kusaka K. On Some Properties of Sintered Stainless Steels at Elevated Temperatures. Powder Metallurgy. 1980; 27(5):2–8.

71. Luiten-Olieman MWJ, Winnubst L, Nijmeijer A, Wessling M, Benes NE. Porous Stainless Steel Hollow Fiber Membranes via Dry-Wet Spinning. Journal of Membrane Science. 2011;370:124-130.

72. Lopez S, Smart DR, Meulenberg S, Diniz Da Costa JC, Wilhelm A. Mixed Matrix Carbon Stainless Steel (MMCSS) Hollow Fibres for Gas Separation. Separation Purification Technology. 2017;174:150-158.

73. Lopez S, Smart DR, Nunes EHM, Vasconcelos D, Vasconcelos WL, Bram M, Meulenberg WA, Diniz Da Costa JC. Stainless Steel Hollow Fibres-Sintering, Morphology and Mechanical Properties. Separation Purification Technology. 2015;147:379-387.

74. Michielsen B, Chen H, Jacobs M, Middelkoop V, Mullens S, Thijs I, Buekenhoudt A, Snijkers F. Preparation of Porous Stainless Steel Hollow Fibers by Robotic Fiber Deposition. Journal of Membrane Science. 2013;437:17-24.

75. Chong JY, Wang B, Li K. High Performance Stainless Steel-Ceramic Composite Hollow Fibres for Microfiltration, Journal of Membrane Science. 2017;541:425-433.

76. Allioux FM, David O, Benavides ME, Kong L, Tanaka DAP, Dumée LF. Preparation of Porous Stainless Steel Hollow-Fibers Through Multi-Modal Particle Size Sintering Towards Pore Engineering. Membranes. 2017;7(3):40.

77. Tan X, Liu S, Li K. Preparation and Characterization of Inorganic Hollow Fiber Membranes. Journal of Membrane Science. 2001;188:87-95.

78. Gohil J. M., Choudhury R. R. Nanoscale Materials in Water Purification. Micro and Nano Technologies. 2019;25-57.

79. Mahon H. E., Creek W.. Permeability Separatory Apparatus, Permeability Separatory Membrane Element, Method of Making the Same and Process. The Dow Cienica Company; 1966.

80. Dzinun H., Dzarfan-Othman M., Ismail A. F. Morphological Study of Co-Extruded Dual-Layer Hollow Fiber Membranes Incorporated with Different TiO_2 Loadings. Journal of Membrane Science. 2015;479:123-131.

81. Ji J, Cecca CD, Schulz EM, Mehta M, Stead D, Mckinley D, Koch DH, Hollow Fibre Membranes and a Method of Making These Membranes. 2005; Patent No. US 6,890.435 B2.

82. Zhang Q, Wang H, Fan X, Chen S, Yu H, Quan X. A Controlled Wet-Spinning and Dip-Coating Process for Preparation of High-Permeable TiO_2 Hollow Fiber Membranes. Water Science Technology. 2016;73(4):725–733.

83. Idris A., Ismail A. F., Noordin M. Y., Shilton S. J.. Optimization of Cellulose Acetate Hollow Fiber Reverse Osmosis Membrane Production Using Taguchi Method. Journal Membrane Science. 2002;205:223-237.

84. Tewfik S. R., Abulnour A. G., Shaalan H. F., El-Anwar M., Ali S., Abed K. A., Badr M. A., Sorour M. H.. Analysis of Some Engineering Parameters Relevant to the Performance and Reliability of Hollow Fiber Spinning System. ARPN Journal of Engineering and Applied Sciences. 2017;12-15.

85. Peng N., Widjojo N,. Sukitpaneenit P., Teoh M. M., Lipscombb G. G., Chung T. S., Lai J. Y.. Evolution of Polymeric Hollow Fibers as Sustainable Technologies: Past, Present, and Future. Progress in Polymer Science. 2012;37(10):1401-1424.

86. Chong K. C., Lai S. O., Thiam H. S., Teoh H. C., Heng S. L.. Recent Progress of Oxygen/Nitrogen Separation Using Membrane Technology. Journal of Engineering Science and Technology. 2016;11(7):1016-1030.

87. Jong J. D., Benes N. E., Koops G. H., Wessling M.. Towards Single Step Production of Multi-Layer Inorganic Hollow Fibers. Journal of Membrane Science. 2004;265-269.

88. Aksoy Y. Gözenekli ve Gözeneksiz Hidrofobik Gaz Transfer Hollow Fiber Membranların Üretimi ve Uygulaması: Fırat Üniversitesi; 2018.

89. Wienk I. M., Boomgaard V. D., Smolders C. A.. The Formation of Nodular Structures in the Top Layer of Ultrafiltration Membranes. Journal Applied Polymer Science. 1994;53:1011-1023.

90. Ahmed S. F.. Preparation and Characterization of Hollow Fiber Nanofiltration Membranes. University of Anbar; 2010.

91. Kutbay I., Kuşkonmaz N.. Mikrodalga Isıtmanın Seramik Üretiminde Kullanımı. Metalurji Dergisi. 2004;52-56.

92. Rui W., Zhang C., Cai C., Gu X.. Effects of Sintering Atmospheres on Properties of Stainless Steel Porous Hollow Fiber Membranes. Journal of Membrane Science. 2015; 489:90–97.

93. Gibson I, Rosen D, Stucker B. Powder Bed Fusion Processes. Additive Manufacturing Technologies. 2015;107-145.

94. Klar E., Samal P.. Powder Metallurgy Stainless Steel: Processing, Microstructure and Properties. ASM International. 2007;1-4.

95. Budin S., Jaafar T.R., Selamat M.A.. Effect of Sintering Atmosphere on the Mechanical Properties of Sintered Tungsten Carbide. MATEC Web of Conferences. 2017;130:03006.

96. Michielsen B., Chen H., Jacobs M.. Preparation of Porous Stainless Steel Hollow Fibers by Robotic Fiber Deposition. Journal of Membrane Science. 2013;437:17–24.

97. Garcia C., Martin F., Tiedra P., Cambronero L. G.. Pitting Corrosion Behaviour of PM Austenitic Stainless Steels Sintered in Nitrogen–Hydrogen Atmosphere. Corrosion Science. 2007;49:1718–1736.

98. Jamaludin I., Abukasim N. A., Mohamadnor N. H., Ismail M. H. Development of Porous Ti-6Al-4V Mix with Palm Stearin Binder by Metal Injection Molding Technique. American Journal of Applied Science. 2015;12(10):742-751.

99. Samal P., Pannell J., Engstrom U., Mars O.. Austenitic Stainless Steels with Enhanced Mechanical Strength. European Powder Metallurgy Association (EPMA). 2010;1–8.

100. Ertugrul O., Park H. S., Onel K., Willert-Porada M.. Structure and Properties of SiC and Emery Powder Reinforced PM 316l Matrix Composites Produced by Microwave and Conventional Sintering. Powder Metallurgy. 2015;41-50.

101. Mariappan R., Kumaran S., Rao T. S.. Effect of Sintering Atmosphere on Structure and Properties of Austeno-Ferritic Stainless Steels. Materials Science and Engineering A. 2009;517(1):328-333.

102. Ayata A.. Toz Metal Aluminium Malzemelerin Mikrodalga Enerjisi ile Sinterlenebilirliğinin Incelenmesi. Gazi Üniversitesi; 2014.

103. Tokita M.. Large Size WC/Co Functionally Graded Materials Fabricated by Spark Plasma Sintering (SPS) Method. Sumitomo Coal Mining Company, Ltd. 2003.

104. Cha S. I., Hong S. H., Kim B. K.. Spark Plasma Sintering Behavior of Nanocrystalline WC-10Co Cemented Carbide Powders. Korea Advanced Institute of Science and Technology; 2002.

105. Sofu M. M., Delikanlı K.. Hızlı Direkt İmalat Yöntemleri Ve Uygulamaları. TİMAK-Tasarım İmalat Analiz Kongresi. 2006;194-200.

106. Kıran K.. Seçici Lazer Ergitme ile Üretilmiş 316L Paslanmaz Çelik Parçaların İnce Tornalama İşlemleri. Süleyman Demirel Üniversitesi; 2011.

107. Matli P. R., Shakoor R. A., Mohamed A. M., Gupta M.. Microwave Rapid Sintering of Al-Metal Matrix Composites: A Review on the Effect of Reinforcements, Microstructure and Mechanical Properties. Metals. 2016;6(7):143.

108. Coovattanachai O., Tosangthum N., Morakotjinda M., Yotkaew T., Krataitong T., Vetayanugul B., Tongsri R.. Effect of Heating Rate on Sintered Series 300 Stainless Steel. Journal Science Technology. 2010;32:163–167.

109.Winston H., Kamalesh S.. Membrane Handbook, Chapman & Hall Ed.. 1992;19-94

110.*Hollow Fiber Membrane Gas Separation*. Federal Aviation Administration Fire Safety. Available from: https://www.fire.tc.faa.gov/systems/fueltank/hfm

111.Rajabi J., Muhamad N., Sulong A. B.. Effect of Nano-Sized Powders on Powder Injection Molding. Microsystem Technology. 2012;18:1941–1961.

112.Oh J.W., Bollina R., Lee W.S., Park S. J.. Effect of Nano Powder Ratio in Bimodal Powder Mixture on Powder Injection Molding. Powder Technology. 2016; 302:168–176.

113.Chong J. Y., Wang B., Li K.. High Performance Stainless Steel-Ceramic Composite Hollow Fibres for Microfiltration. Journal of Membrane Science. 2017;541:425–433.

114.Luiten-Olieman M., Winnubst L., Nijmeijer A., Wessling M., Nieck E. Porous Stainless Steel Hollow Fiber Membranes via Dry–Wet Spinning. Benes Journal of Membrane Science. 2011;370:124–130.

115.Michielsen B., Chen H., Jacobs M.. Preparation of Porous Stainless Steel Hollow Fibers by Robotic Fiber Deposition. Journal Membrane Science. 2013;437:17-24.

116.Schmeda-Lopez D., Smart S., Eduardo H. M., Vasconcelos D., Vasconcelos W. M., Meulenberg W., Diniz Da Costa J.. Stainless Steel Hollow Fibres-Sintering, Morphology and Mechanical Properties. Separation and Purification Technology. 2015;381-389.

117.Oliveira S. S., Ferreira B., Lira H., Santana L., Araújo E. M.. Development of Hollow Fiber Membranes with Alumina and Waste of Quartzite. Materials Research. 2019;0171.

118.Zhong Q., Xu Z. L., Ma X., Wang. M.. Modification of Porous Stainless Steel Hollow Fibers by Adding TiO_2, ZrO_2 and SiO_2 Nano Particles. Journal of Porous Materials. 2016;23(3):1529-1536.

119.Li H., Song J., Tan X., Jin Y., Liu S.. Preparation of Spiral Porous Stainless Steel Hollow Fiber Membranes by A Modified Phase Inversion–Sintering Technique. Journal of Membrane Science. 2015;489:292–298

CURRICULUM VITAE

Name Surname: EZGİ ŞAHİN

Place and Date of Birth: Eskişehir - 21.08.1995

Education

- The Master of Science (MSc): İzmir Kâtip Çelebi University, Faculty of Engineering and Architecture, Materials Science and Engineering (100% English), (2018 – 2021).
- The Bachelor of Science (BSc): İzmir Kâtip Çelebi University, Faculty of Engineering and Architecture, Materials Science and Engineering (100% English), (2013 – 2018).

Professional Experience and Rewards

- TÜBİTAK (The Scientific and Technological Research Council of Turkey), BİLGEM (Informatics and Information Security Research Center) – Researcher, (2019 - …)
- Honor Award (Ranking 1st in department), (2018)

Publications and Presentations

- O. Ertuğrul, Z. Ç. Öter, M. S. Yılmaz, E. Şahin, M. Coşkun, G. Tarakçı, E. Koç, "Effect of HIP process and subsequent heat treatment on microstructure and mechanical properties of direct metal laser sintered AlSi10Mg alloy", Rapid Prototyping Journal, (DOI 10.1108/RPJ-07-2019-0180), (2020), (Article)
- Ezgi Şahin, Onur Ertuğrul, Özgün Yücel, Production and Characterization of Zircon Based Hollow Fiber Membranes, Porous and Powder Materials Symposium and Exhibition, (2019), (Presentation by Ezgi Şahin and proceedings paper)
- Ezgi Şahin, Onur Ertuğrul, Özgün Yücel, Production of Stainless Steel Hollow Fiber Membranes by Microwave and Conventional Sintering and Their Detailed Characterization, Porous and Powder Materials Symposium and Exhibition, (2019), (Presentation by Ezgi Şahin and abstract paper)
- Ezgi Şahin, Büşra Beşli, Çağlar Erdem, Ahmet Aykaç, Fethullah Güneş, Mustafa Erol, Evren Çulcular, Synthesis of 2D Graphene Decorated with Gold Nanoparticles, 2nd International Students Science Congress, (2018), (Presentation by Ezgi Şahin and proceedings paper)